

INFERENCE FOR MULTIPLE TREATMENT EFFECTS USING CONFOUNDER IMPORTANCE LEARNING

OMIROS PAPASPILIOPOULOS ¹, DAVID ROSSELL ²,
AND MIQUEL TORRENS-DINARÈS ³

ABSTRACT. We address modelling and computational issues for multiple treatment effect inference under many potential confounders. A primary issue relates to preventing harmful effects from omitting relevant covariates (under-selection), while not running into over-selection issues that introduce substantial variance and a bias related to the non-random over-inclusion of covariates. We propose a novel empirical Bayes framework for Bayesian model averaging that learns from data the extent to which the inclusion of key covariates should be encouraged, specifically those highly associated to the treatments. A key challenge is computational. We develop fast algorithms, including an Expectation-Propagation variational approximation and simple stochastic gradient optimization algorithms, to learn the hyper-parameters from data. Our framework uses widely-used ingredients and largely existing software, and it is implemented within the R package `mombf` featured on CRAN. This work is motivated by and is illustrated in two applications. The first is the association between salary variation and discriminatory factors. The second, that has been debated in previous works, is the association between abortion policies and crime. Our approach provides insights that differ from previous analyses especially in situations with weaker treatment effects.

Keywords: multiple treatment effects, Bayesian model averaging, empirical Bayes, variational approximation

1: Bocconi University, omiros@unibocconi.it.

2: Pompeu Fabra University, david.rossell@upf.edu.

3: Centre for Genomic Regulation, miquel.torrens@crg.eu.

1. INTRODUCTION

We consider a problem of fundamental importance in applied research, that of evaluating the joint effect, if any, of multiple treatments on a response variable when working with observational data and when there are many potential adjustment covariates. We also showcase two applications. One is the association between salary variation and discriminating factors such as gender, race and country of birth, and how this has evolved over time. Another example relates to a debate on a possible association between planned parenthood (as measured by abortion rates) and crime.

Our upcoming discussion is already relevant when the goal is to simply study conditional associations between outcome and treatments (given the covariates). It however becomes critical for causal inference, whereby relying on the so-called non-interference and no unmeasured confounding assumptions, one may identify causal treatment effects from a regression model, provided one selects the necessary covariates (see [Antonelli and Dominici \[2021\]](#) for a recent review). Following standard terminology, we refer by *confounders* to covariates that are directly associated with both treatment(s) and the response, and by *instruments* to covariates that correlate with the treatment(s) but are conditionally independent of the outcome, given the treatment(s). Briefly, inferring treatment effects using observational data is subject to selection biases and unmeasured confounding, hence it is important to consider a large number of covariates and to select a suitable subset thereof. It is also important to allow for interaction terms and other transformations, such as polynomial or spline terms to obtain a flexible model and account for possible heterogeneous effects [[Caron et al., 2022](#)]. As a result, a popular approach to treatment effect inference is to use high-dimensional regression techniques, and we pursue this direction in this article. To put matters in perspective, our analysis of salary variation involves four treatments and hundreds of covariates, and we consider treatment effect heterogeneity across states, whereas for the crime data we have one treatment and 295 covariates.

We model the dependence of the response $y_i \sim p(y_i; \eta_i, \phi)$ on $t = 1, \dots, T$ treatments $d_{i,t}$ and $j = 1, \dots, J$ covariates $x_{i,j}$, via

$$(1) \quad \eta_i = \sum_{t=1}^T \alpha_t d_{i,t} + \sum_{j=1}^J \beta_j x_{i,j}, i = 1, \dots, n$$

where $p(y_i; \eta_i, \phi)$ defines a generalized linear model with linear predictor η_i and dispersion parameter ϕ (i.e. the error variance in the Gaussian case, and a known $\phi = 1$ in logistic and Poisson regression models). Whereas from an interpretational and policy making point of view the distinction between treatments and covariates is clear, statistically the difference is one of priorities: we are primarily interested

in inference for the former, i.e the set of α_t 's in (1), including uncertainty quantification such as high probability intervals for α_t , whereas the latter are considered for potential inclusion to avoid omitted variable biases and to allow for flexible regression functions. Although our primary interest is in average treatment effects, it is possible to consider heterogeneous treatment effects by incorporating into $d_{i,t}$ interactions between treatments and covariates. In our salary example we illustrate this by considering interactions between the four primary treatments and state. Importantly, such interactions are added with an add-to-zero constraint. This ensures that the α_t associated to a primary treatment quantifies its corresponding average treatment effect, whereas the α_t 's associated to interactions quantify deviations from the average treatment effect.

Our main interest is in scenarios where the number of covariates J is large. This setting spurred significant interest due to the observation that standard shrinkage and selection methods for learning (1), such as LASSO and Bayesian Model Averaging (BMA), can have an undesirable behavior for treatment effect inference. Intuitively, when some confounders are strongly associated with the treatments, standard high-dimensional methods may fail to include said confounders (or even the treatments) in (1), resulting in significant omitted variable biases in estimating the treatment effects. Two seminal works where these issues are discussed and addressed are Belloni et al. [2014] and Wang et al. [2012]. Both works arguably set the basis for subsequent literature, and both consider a single treatment setting ($T = 1$). Belloni et al. [2014] proposed a double-LASSO (DL) approach where one regresses separately the response and the treatment on the covariates via the LASSO, takes the covariates with a non-zero estimated effect either on the treatment or the response, and in a second step fits a model like (1) by OLS with these selected covariates. Notably, this treatment effect estimator is asymptotically normally-distributed and has a variance that can be estimated from data. In a similar spirit Wang et al. [2012] proposed Bayesian adjustment for confounders (BAC), which models jointly the response and treatments and uses a prior distribution that encourages covariates to be simultaneously selected in the two regression models.

The main idea in DL, BAC and much of the subsequent literature (reviewed below) is that, by including covariates that are associated to the treatment, one ameliorates omitted variable biases. A key issue motivating our work is that, by protecting oneself against covariate under-selection, one may force (or encourage) the inclusion of instruments, i.e. covariates for which $\beta_j = 0$ in (1). Under such covariate over-selection treatment effects remain identifiable, however it leads to a problematic *variance inflation*, see De Luna et al. [2011], Lefebvre

et al. [2014], Talbot et al. [2015], Henckel et al. [2022]. Adding instruments can severely inflate the treatment effect mean squared error (MSE), and reduce the power to detect weaker effects. To gain intuition, consider a setting with a fixed number of covariates J . There, a classical strategy is to fit one model including all covariates to obtain unbiased treatment effects, potentially at the cost of high variance. Specifically, the variance inflation factor for a least-squares estimator of α_t is given by $(1 - R_t^2)^{-1}$, where R_t is the multiple R^2 coefficient for regressing treatment t on the covariates. Belloni et al. [2014] explain that, when J is fixed, their approach is asymptotically first-order equivalent to fitting a model with all covariates, and hence incurs the mentioned variance inflation factor. A second issue is a more subtle, and to the best of our knowledge yet unnoticed, *over-selection bias*. Namely, that the inclusion of covariates in (1) which are screened out to be correlated with the treatments and the response may lead to biased inference for the treatment effects. In our experience said over-selection bias is not a major issue in practice, further the results in Belloni et al. [2014] prove that it vanishes asymptotically, hence we defer further discussion to Section D.

Related literature includes Farrell [2015], who adapted the DL framework by using a robust estimator to safeguard from mistakes in the double selection step, and Shortreed and Ertefaie [2017], who employed a two-step adaptive LASSO approach. Chernozhukov et al. [2018] extended DL by introducing a de-biasing step, and cross-fitting to ameliorate false positive inclusion of covariates. As an alternative to these two-step approaches, Ertefaie et al. [2015] used a joint likelihood L_1 penalization on the outcome and treatment regressions. On the Bayesian side, Lefebvre et al. [2014] discussed how to set the BAC hyper-parameter ω in a data-based manner to improve the treatment effect MSE. When $\omega = \infty$, the outcome equation includes any covariate associated with the treatment, which akin to DL reduces omitted variable bias at the cost of potentially inflating MSE. The authors warn that the results are sensitive to using 1/2 of the data in their sample-splitting strategy, and of computational challenges if one wanted to consider $T > 1$ treatments, further they use a leaps-and-bounds model search that only accommodates up to 31 covariates. Wang et al. [2015] extended BAC to generalized linear models and considered pairwise interactions between the treatment and covariates. The authors used the same prior as BAC and focused on the hyper-parameter choice $\omega = \infty$, which as discussed can be problematic. Talbot et al. [2015] propose a similar framework to BAC where prior probabilities deter the inclusion of instruments to reduce the inclusion of instruments, however said prior probabilities still require a tuning hyper-parameter playing a role similar to ω in BAC. A proposal related to ours is the ACPME method of Wilson et al. [2018]. The framework considers $T > 1$ treatments

and the prior inclusion probability for covariate j depends, via logistic regression, on a measure of dependence between j and the treatments. Said measure is given by regressing the controls on the treatments and taking the corresponding residual covariance matrix. Analogously to BAC, prior inclusion probabilities are controlled by a tuning parameter, which by default is set such that the average penalty for covariate inclusion is the same as that for the Bayesian information criterion. Antonelli et al. [2019] proposed continuous spike-and-slab Laplace priors on high-dimensional covariates. The framework is designed to reduce the shrinkage to zero of the coefficients of covariates that are associated to the treatment. They discuss how to elicit hyper-parameter values to help shrink the effects of instruments. In a different thread, Hahn et al. [2018] proposed a shrinkage prior framework based on reparameterizing a joint outcome and treatment regression, designed to improve estimation biases, and Hahn et al. [2020] considered Bayesian causal forests. Overall, a recurrent issue in the Bayesian literature is how to set hyper-parameter values such that one includes all confounders and hence identifies the treatment effects, while preventing variance inflation due to selecting instruments.

Our main contributions are proposing a novel Bayesian model, and an associated computational framework, to learn hyper-parameters that determine whether and how prior covariate inclusion probabilities should relate to their association with the treatments. Our framework, to which we refer by Confounder Importance Learning (CIL), is designed to deal with both over- and under-selection, in both high and low confounding situations. Figure 1 is a first illustration of its merits (see Section 4.1 for details). As discussed in Belloni et al. [2014] and Wang et al. [2012], due to under-selection bias standard LASSO and BMA suffer from high MSE in high-confounding settings, whereas their proposed DL and BAC (respectively) attain much lower MSE. In low-confounding settings however the reverse is true, here DL and BAC have high MSE due to over-selection variance. CIL attains low MSE across the weak-to-strong confounding spectrum. CIL can also consider multiple treatments, a setting that has received less attention in the literature. Our model has similarities to that in ACPME, the key difference being that we learn hyper-parameters from the data (and subtler differences discussed in Section 2). However, in Figure 1 we observe that the two methods show different result patterns in the single treatment case, as ACPME closely mimics the behavior of BAC across the board. Relative to Lefebvre et al. [2014], we learn hyper-parameters using the marginal likelihood associated to a Bayesian model rather than a training-test data split. A key ingredient relative to earlier proposals are two scalable computational algorithms, one based on MCMC and the other on a variational approximation. In principle evaluating

the (log) marginal likelihood requires a costly sum over 2^{T+J} models. We show that, under our proposed prior model, its gradient only requires a sum over J terms that involves only marginal posterior inclusion probabilities. We further propose an expectation-propagation (EP) approximation that bypasses the need to re-estimate said marginal posterior probabilities, which would typically require MCMC. For example, BAC and ACPME failed to return a solution in our salary example after 2 days, whereas our CIL could complete the task in 8 hours and 33 minutes on the largest dataset of 2010. CIL can be easily implemented using existing software, and we provide an implementation within the R package `mombf` [Rossell et al., 2023].

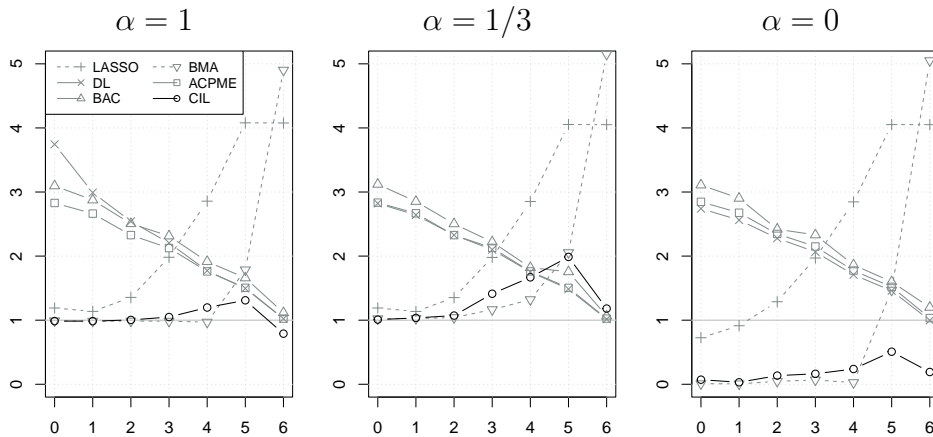


FIGURE 1. Parameter root MSE relative to an oracle OLS, for a single treatment, considering strong ($\alpha = 1$), weak ($\alpha = 1/3$) and no effect ($\alpha = 0$). In all panels, $n = 100$, $J = 49$ and the response and treatment are simulated from a linear regression model based on 6 active covariates each. The x -axis is the overlap between the two sets of active covariates varies from 0 (no confounding) to 6 (full confounding). DL is double LASSO, BMA is Bayesian model averaging, BAC is Bayesian Adjustment for Confounding and CIL is Confounder Importance Learning

The remainder of paper is structured as follows. Section 2 details our proposed approach, a Bayesian model averaging where prior inclusion probabilities vary across covariates. Section 3 describes our computational methods. Section 4 shows a simulation study illustrating that standard high-dimensional methods have high MSE in high-confounding settings, whereas other methods designed for treatment effect inference have high MSE in low-confounding settings, and that

CIL attains a good MSE throughout. We also apply the methodology to the salary and crime case studies. We illustrate how considering multiple treatments allows to portray, via posterior predictive inference, a measure of joint salary variation due to potentially discriminatory factors. All proofs and additional empirical results are provided as a supplement.

2. MODELLING FRAMEWORK

We model the dependence of the response y_i on treatments $\mathbf{d}_i = (d_{i,1}, \dots, d_{i,T})$ and covariates $\mathbf{x}_i = (x_{i,1}, \dots, x_{i,J})$, according to (1). We are primarily interested in inference for the treatment effects $\boldsymbol{\alpha} = (\alpha_1, \dots, \alpha_T)$. We adopt a Bayesian framework where we introduce variable inclusion indicators $\gamma_j = \mathbb{I}(\beta_j \neq 0)$ and $\delta_t = \mathbb{I}(\alpha_t \neq 0)$, and define a prior

$$(2) \quad p(\boldsymbol{\alpha}, \boldsymbol{\beta}, \boldsymbol{\delta}, \boldsymbol{\gamma}, \phi \mid \boldsymbol{\theta}) = p(\boldsymbol{\alpha}, \boldsymbol{\beta} \mid \boldsymbol{\delta}, \boldsymbol{\gamma}, \phi) p(\boldsymbol{\gamma} \mid \boldsymbol{\theta}) p(\boldsymbol{\delta}) p(\phi),$$

where $\boldsymbol{\theta}$ are hyper-parameters discussed below, and $p(\phi)$ is dropped for models with known dispersion parameter (e.g. logistic or Poisson regression). For the regression coefficients, we assume prior independence,

$$p(\boldsymbol{\alpha}, \boldsymbol{\beta} \mid \boldsymbol{\delta}, \boldsymbol{\gamma}, \phi) = \prod_{t=1}^T p(\alpha_t \mid \delta_t, \phi) \prod_{j=1}^J p(\beta_j \mid \gamma_j, \phi).$$

We remark that much of the Bayesian treatment literature does not consider treatment inclusion indicators, rather they are forced into the model. While that strategy is easily accommodated in our framework by setting $\delta_t = 1$ for all t , we consider that one often wishes to assess whether the treatment effects exist in the first place, and otherwise shrink their estimates towards zero. Accordingly with this goal, we adopt the so-called product moment (pMOM) non-local prior of [Johnson and Rossell \[2012\]](#). Briefly, non-local priors improve the rates at which one discards the truly zero parameters, see [Johnson and Rossell \[2012\]](#), [Wu \[2016\]](#), [Shin et al. \[2018\]](#), [Rossell \[2021\]](#). Under the pMOM prior, one has $\alpha_t = 0$ almost surely if $\delta_t = 0$, and

$$p(\alpha_t \mid \delta_t = 1, \phi) = \frac{\alpha_t^2}{\phi\tau/v_t} \text{N}(\alpha_t; 0, \phi\tau/v_t),$$

with the analogous setting for every β_j . [Figure 8](#) illustrates its density. Above v_t is the sample variance of treatment t , to ease notation we assume that treatments and covariates have unit variance and take $v_t = 1$. The pMOM prior involves a prior dispersion parameter $\tau > 0$, that by default we set to $\tau = 1/3$ following [Rossell et al. \[2021\]](#), which leads to a minimally informative prior akin to the unit information prior underlying the Bayesian information criterion. As for the dispersion

parameter, where unknown, we also place a minimally informative $\phi \sim \text{IGam}(0.01, 0.01)$ prior.

For the inclusion indicators, we assume prior independence, and set

$$(3) \quad p(\boldsymbol{\delta}, \boldsymbol{\gamma} \mid \boldsymbol{\theta}) = \prod_{t=1}^T \text{Bern}(\delta_t; 1/2) \prod_{j=1}^J \text{Bern}(\gamma_j; \pi_j(\boldsymbol{\theta})).$$

All treatments get a fixed marginal prior inclusion probability $P(\delta_t = 1) = 1/2$, as we do not want to favor their exclusion a priori, considering that there is at least some suspicion that any given treatment has an effect. This choice is a practical default when the number of treatments T is not too large, else one may set $P(\delta_t = 1) < 1/2$ to avoid false positive inflation due to multiple hypothesis testing [Scott and Berger, 2010, Rossell, 2021]. Our software allows such possibilities.

The main modelling novelty in this article is the choice of covariate prior inclusion probabilities $\pi_j(\boldsymbol{\theta}) = P(\beta_j \neq 0 \mid \boldsymbol{\theta})$, where $\boldsymbol{\theta} = (\theta_0, \theta_1, \dots, \theta_T)$ is a key prior hyper-parameter relating $\pi_j(\boldsymbol{\theta})$ to (positive) measures of association $\mathbf{f}_j = (f_{j,1}, \dots, f_{j,T})$ between covariate j and the T treatments. Specifically,

$$(4) \quad \pi_j(\boldsymbol{\theta}) = \rho + (1 - 2\rho) \left(1 + \exp \left\{ -\theta_0 - \sum_{t=1}^T \theta_t f_{j,t} \right\} \right)^{-1}$$

where $\rho \in (0, 1/2)$. Model (4) is essentially that used in logistic regression where the scalar ρ ensures that prior inclusion probabilities $\pi_j(\boldsymbol{\theta}) \in [\rho, 1 - \rho]$ are bounded away from (0,1), so that one does not include/exclude covariates a priori. We propose the default $\rho = 1/(J^2 + 1)$, which sets a lower-bound $P(\beta_j \neq 0 \mid \boldsymbol{\theta}) \geq 1/(J^2 + 1)$ that is of the same order as J grows as the complexity priors in Castillo and van der Vaart [2012]. These bounds on the prior inclusion probabilities ensure that one may consistently recover the true model as $n \rightarrow \infty$, assuming suitable conditions, see Rossell [2021] for a detailed discussion.

Akin to DL, BAC and related methods, the idea is that if covariate j is highly associated to treatment t then $f_{j,t}$ will be large, and if $\theta_t > 0$ then one favors the inclusion of such covariates. In contrast, if $\theta_t = 0$ then said inclusion is not encouraged, and if $\theta_t < 0$ it is discouraged. Figure 2 illustrates $\pi_j(\boldsymbol{\theta})$ for three different values of θ_1 . Setting $\boldsymbol{\theta}$ is critical for the performance of our inferential paradigm, and in Section 3 we introduce data-driven criteria and algorithms for its choice. Intuitively, in high-confounding scenarios where covariates associated to treatment t are also associated to the outcome, one expects to learn $\theta_t > 0$. In contrast, in low-confounding scenarios where most covariates associated to treatment t are instruments, one expects to learn $\theta_t < 0$.

Our generic approach is to take $f_{j,t} = |w_{j,t}|$, where $\mathbf{w}_t = (w_{1,t}, \dots, w_{J,t})$ are regression coefficients obtained via a high-dimensional regression

of \mathbf{d}_t on the covariates. The idea is that covariates with large $f_{j,t}$ are likely to be parents (in a generative directed graphical model that describes the whole system) of treatment t , and that including parents of the treatment ensures satisfying Pearl’s backdoor criterion and hence identifying the treatment effects. Although our framework allows the user to specify any suitable $f_{j,t}$, here we highlight two possible choices. First, a LASSO regression,

$$(5) \quad \mathbf{w}_t := \arg \min_{(v_{t,1}, \dots, v_{t,J})} \left\{ \sum_{i=1}^n \log p \left(d_{i,t}; \sum_{j=1}^J x_{i,j} v_{t,j} \right) + \lambda \sum_{j=1}^J |v_{t,j}| \right\},$$

where $\lambda > 0$ is a regularization parameter, which we set by minimizing the BIC (we obtained similar results when using cross-validation). The choice in (5) balances speed with reasonable point estimate precision, and is the option that we used in all our examples. A second option, available when dealing with continuous treatments, is to use the minimum norm ridge regression,

$$(6) \quad \mathbf{w}_t = (\mathbf{X}^T \mathbf{X})^+ \mathbf{d}_t,$$

where $(\mathbf{X}^T \mathbf{X})^+$ is the Moore-Penrose pseudo-inverse, and \mathbf{X} the $n \times J$ design matrix. For $J < n$ this is the familiar OLS estimator, but (6) is also well-defined when $J > n$, and it has been recently investigated in terms of the so-called benign overfitting property in [Bartlett et al. \[2020\]](#). [Wang and Leng \[2016\]](#) showed that when $J > n$, (6) ranks the coefficients consistently under theoretical conditions slightly broader than the LASSO. Therefore, one expects that all parents of treatment t have larger values of $f_{j,t}$. Similarly, by the screening property of the LASSO one expects that all parents of treatment t have $f_{j,t} = |w_{j,t}| > 0$. This is appealing in our context, since $\pi_j(\boldsymbol{\theta})$ are mainly driven by the relative magnitudes of $f_{j,t}$, the prior inclusion probabilities are allowed to favor or discourage the parents of treatments (depending on whether $\theta_t > 0$ or $\theta_t < 0$). Recall that DL, BAC and most of the literature is based on encouraging the inclusion of such covariates, which would be harmful in low-confounding scenarios.

We remark that in the ACPME framework of [Wilson et al. \[2018\]](#) one also pre-computes features relating treatments to covariates. Relative to BAC, pre-computing features offers a massive computational simplification, since no model search over treatment equations is needed (which would multiply the model space size by 2^{JT}). Relative to ACPME, we measure treatment-covariate association by regressing the treatments on the controls, rather than regressing the controls on the treatments. We opted for the former option because one needs to run T rather than J regressions, and that as discussed this allows consistently identifying parents of the treatments as n grows. Further, as discussed next, we propose learning our hyper-parameters $\boldsymbol{\theta}$ using likelihood-based methods, and propose scalable computational algorithms to do

so. In Section 4 we show comparisons between our CIL, BAC, ACPME, and other methods.

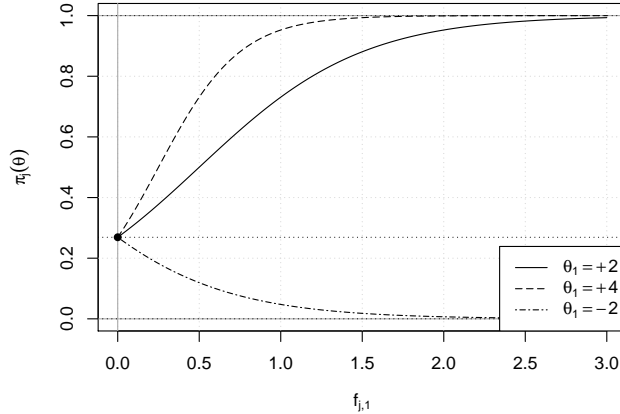


FIGURE 2. Prior inclusion probability (4) as a function of $f_{j,1}$, a feature measuring correlation between covariate j and treatment $t = 1$, for $\theta_0 = -1$, $\rho = (J^2 + 1)^{-1}$, and $J = 99$ covariates. Top and bottom dotted lines show the upper and lower bounds, $1 - \rho$ and ρ , respectively. The dotted line in the middle corresponds to $\theta_1 = 0$.

3. COMPUTATIONAL METHODOLOGY

3.1. Bayesian model averaging. All expressions in this section are conditional on the observed $(\mathbf{x}_i, \mathbf{d}_i)$, we drop them from the notation for simplicity. Inference for our approach relies on posterior model probabilities

$$p(\boldsymbol{\gamma}, \boldsymbol{\delta} \mid \mathbf{y}, \boldsymbol{\theta}) \propto p(\mathbf{y} \mid \boldsymbol{\gamma}, \boldsymbol{\delta})p(\boldsymbol{\gamma} \mid \boldsymbol{\theta})p(\boldsymbol{\delta}),$$

where

$$(7) \quad p(\mathbf{y} \mid \boldsymbol{\gamma}, \boldsymbol{\delta}) = \int p(\mathbf{y} \mid \boldsymbol{\alpha}, \boldsymbol{\beta}, \phi, \boldsymbol{\delta}, \boldsymbol{\gamma})p(\boldsymbol{\alpha}, \boldsymbol{\beta} \mid \boldsymbol{\delta}, \boldsymbol{\gamma}, \phi)p(\phi)d\boldsymbol{\alpha}d\boldsymbol{\beta}d\phi$$

is the marginal likelihood of model $(\boldsymbol{\gamma}, \boldsymbol{\delta})$. We set the hyper-parameter $\boldsymbol{\theta}$ to a point estimate $\hat{\boldsymbol{\theta}}$ described in Sections 3.2-3.3. Conditional on $\boldsymbol{\theta}$, our model prior $p(\boldsymbol{\gamma} \mid \boldsymbol{\theta})$ is a product of independent Bernoulli's with asymmetric success probabilities defined by (4). As a simple variation of standard BMA, one can exploit existing computational algorithms, which we outline next.

Outside particular cases such as Gaussian regression under Gaussian priors, (7) does not have a closed-form expression. To estimate (7) under our pMOM prior we adopt the approximate Laplace approximations of Rossell et al. [2021], see Section G.1 for an overview. We then

obtain point estimates using BMA,

$$(8) \quad \hat{\alpha} := \sum_{\gamma, \delta} E(\alpha \mid \mathbf{y}, \gamma, \delta) p(\gamma, \delta \mid \mathbf{y}, \boldsymbol{\theta}),$$

and similarly we employ the BMA posterior density $p(\alpha \mid \mathbf{y}, \gamma, \delta, \boldsymbol{\theta})$ to provide posterior credible intervals. To this end we use posterior samples from the pMOM posterior density using a latent truncation representation described by [Russell and Telesca \[2017\]](#). Expression (8) is a sum across 2^{T+J} models, when it is unfeasible we use Markov Chain Monte Carlo to explore the posterior distribution $p(\gamma, \delta \mid \mathbf{y}, \boldsymbol{\theta})$, see e.g. [Clyde and Ghosh \[2012\]](#) for a review.

We used all the algorithms described above as implemented by the `cil` function in R package `mombf` [[Russell et al., 2023](#)].

3.2. Confounder importance learning via marginal likelihood.

Our main computational contribution is a strategy to learn the hyper-parameter $\boldsymbol{\theta}$, which plays a critical role by determining prior inclusion probabilities. Below we devise an empirical Bayes approach and a variational approximation thereof.

The starting point is the marginal likelihood,

$$p(\mathbf{y} \mid \boldsymbol{\theta}) = \sum_{\delta, \gamma} p(\mathbf{y} \mid \delta, \gamma) p(\delta, \gamma \mid \boldsymbol{\theta}),$$

with the first term inside the sum given in (7). The empirical Bayes estimator is $\boldsymbol{\theta}^{\text{EB}} = \arg \max_{\boldsymbol{\theta}} p(\mathbf{y} \mid \boldsymbol{\theta})$ and its use for hyper-parameter learning in variable selection has been well-studied, see [George and Foster \[2000\]](#), [Scott and Berger \[2010\]](#), [Petroni et al. \[2014\]](#). We remark that it is possible to add a prior $p(\boldsymbol{\theta})$ and use the marginal posterior modal estimate $\boldsymbol{\theta}^{\text{EB}} = \arg \max_{\boldsymbol{\theta}} p(\mathbf{y} \mid \boldsymbol{\theta}) p(\boldsymbol{\theta})$, however in our experiments this did not lead to noticeable differences in the results.

The main challenge in obtaining $\boldsymbol{\theta}^{\text{EB}}$ is that evaluating $p(\mathbf{y} \mid \boldsymbol{\theta})$ requires a costly sum over (δ, γ) . Fortunately, it is possible to obtain a simpler expression for the gradient of the log-marginal likelihood, given in [Proposition 3.1](#). The proof (see [Section A](#)) leverages the fact that \mathbf{y} is conditionally independent from $\boldsymbol{\theta}$ given (γ, δ) , that the prior $p(\delta, \gamma \mid \boldsymbol{\theta})$ factorizes, and the specific form of $\pi_j(\boldsymbol{\theta})$ in (4).

Proposition 3.1. *For our model as defined in (1), (2), (3) and (4) we obtain that*

$$(9) \quad \nabla_{\boldsymbol{\theta}} \log p(\mathbf{y} \mid \boldsymbol{\theta}) = (1 - 2\rho) \sum_{j=1}^J \mathbf{f}_j [P(\gamma_j = 1 \mid \mathbf{y}, \boldsymbol{\theta}) - \pi_j(\boldsymbol{\theta})],$$

where $\mathbf{f}_j = (1, f_{j,1}, \dots, f_{j,T})^\top$.

Proposition 3.1 allows using gradient-based optimization to approximate $\boldsymbol{\theta}^{\text{EP}}$. Notice that we only need to sum over J terms, as opposed to 2^{J+T} for evaluating the marginal likelihood, and the gradient only depends on the data via the marginal inclusion probabilities $P(\gamma_j = 1 \mid \mathbf{y}, \boldsymbol{\theta})$, which can typically be estimated more accurately than joint model probabilities. However, one must still compute $P(\gamma_j = 1 \mid \mathbf{y}, \boldsymbol{\theta})$ for every considered $\boldsymbol{\theta}$, which is intensive when the optimization requires more than a few iterations, since typically an MCMC algorithm will be used to estimate these probabilities. We next describe an Expectation Propagation variational approximation which, as illustrated in Figure S4, typically provides a good approximation to the global mode.

3.3. Confounder importance learning by Expectation-Propagation.

The use of Expectation Propagation (EP) [Minka, 2001a,b] is common in machine learning, including in variable selection [Seeger et al., 2007, Hernández-Lobato et al., 2013, Xu et al., 2014]. We propose a computationally efficient approximation to the marginal likelihood optimizer that can be used as is, or serve as initialization for a the gradient-based optimization discussed in Section 3.2. We comment on our experience with both schemes later in this section.

To simplify notation, we first define the posterior inclusion probabilities for a specific value of $\boldsymbol{\theta}$:

$$p_0(\boldsymbol{\delta}, \boldsymbol{\gamma} \mid \mathbf{y}) = p(\boldsymbol{\delta}, \boldsymbol{\gamma} \mid \mathbf{y}, \boldsymbol{\theta} = \mathbf{0}) \propto p(\mathbf{y} \mid \boldsymbol{\delta}, \boldsymbol{\gamma}).$$

the right-hand side following from the fact that, when $\boldsymbol{\theta} = \mathbf{0}$, the prior on the model space $p(\boldsymbol{\delta}, \boldsymbol{\gamma} \mid \boldsymbol{\theta} = \mathbf{0}) = 1/2^{J+T}$ is the uniform distribution. We consider a mean-field approximation to $p_0(\boldsymbol{\delta}, \boldsymbol{\gamma} \mid \mathbf{y})$,

$$(10) \quad q(\boldsymbol{\delta}, \boldsymbol{\gamma}) = \prod_{t=1}^T \text{Bern}(\delta_t; s_t) \prod_{j=1}^J \text{Bern}(\gamma_j; r_j).$$

where $\mathbf{s} = (s_1, \dots, s_T)$ and $\mathbf{r} = (r_1, \dots, r_J)$ are variational parameters, which EP chooses by minimizing a Kullback-Leibler divergence, as given in Proposition 3.2.

Proposition 3.2. *The parameters that minimize the Kullback-Leibler divergence between p_0 and q ,*

$$(11) \quad (\mathbf{r}^{\text{EP}}, \mathbf{s}^{\text{EP}}) = \arg \max_{\mathbf{r}, \mathbf{s}} \sum_{\boldsymbol{\gamma}, \boldsymbol{\delta}} p_0(\boldsymbol{\delta}, \boldsymbol{\gamma} \mid \mathbf{y}) \log \left(\frac{p_0(\boldsymbol{\delta}, \boldsymbol{\gamma} \mid \mathbf{y})}{q(\boldsymbol{\delta}, \boldsymbol{\gamma})} \right).$$

are given by

$$(12) \quad r_j^{\text{EP}} = P_0(\gamma_j = 1 \mid \mathbf{y}), \quad s_t^{\text{EP}} = P_0(\delta_t = 1 \mid \mathbf{y}).$$

The way we propose to use this approximation for a computationally inexpensive estimator of $\boldsymbol{\theta}$ is as follows. First, note that

$$(13) \quad p(\mathbf{y} \mid \boldsymbol{\theta}) = \sum_{\boldsymbol{\delta}, \boldsymbol{\gamma}} p(\mathbf{y} \mid \boldsymbol{\delta}, \boldsymbol{\gamma}) p(\boldsymbol{\delta}, \boldsymbol{\gamma} \mid \boldsymbol{\theta}) \propto \sum_{\boldsymbol{\delta}, \boldsymbol{\gamma}} p_0(\boldsymbol{\delta}, \boldsymbol{\gamma} \mid \mathbf{y}) p(\boldsymbol{\delta}, \boldsymbol{\gamma} \mid \boldsymbol{\theta}).$$

Our strategy is to replace p_0 by q , using the optimized variational parameters in Proposition 3.2, which reduces the above sum from one over 2^{J+T} terms to one over J terms. Specifically, it is possible to show that (see Section E.1) this leads to

$$(14) \quad \boldsymbol{\theta}^{\text{EP}} = \arg \max_{\boldsymbol{\theta}} \sum_{j=1}^J \log (r_j^{\text{EP}} \pi_j(\boldsymbol{\theta}) + (1 - r_j^{\text{EP}})(1 - \pi_j(\boldsymbol{\theta}))) .$$

Our strategy is to pre-compute $r_j^{\text{EP}} = P(\gamma_j = 1 \mid \mathbf{y}, \boldsymbol{\theta} = \mathbf{0})$, prior to conducting the optimization in (14). This leads to an optimization over $\boldsymbol{\theta} \in \mathbb{R}^{T+1}$ where, in contrast to the marginal likelihood estimate $\boldsymbol{\theta}^{\text{EB}}$, the objective function can be cheaply evaluated. Since the function in (14) is not concave, we conduct an initial grid search and subsequently use a quasi-Newton algorithm, see Algorithm 1 in the supplement. Although this was not an issue in our examples, when the number of treatments T is large the mentioned grid search becomes too costly. Possible alternatives are either using Bayesian optimization methods or simply initializing at $\boldsymbol{\theta} = \mathbf{0}$ (uniform model prior) and using the gradient of the objective function in (14), which we give in Section E.2.

In our examples $\boldsymbol{\theta}^{\text{EB}}$ and $\boldsymbol{\theta}^{\text{EP}}$ provided virtually indistinguishable inference, the latter incurring a significantly lower computational cost. Figure 9 shows a comparison for one of our simulated datasets. On the other hand, $\boldsymbol{\theta}^{\text{EB}}$ does provide slight advantages in some settings where the number of parameters $J + T$ was particularly large (see Section 4.1).

4. RESULTS

In Section 4.1 we present a series of simulation studies, where we aim to illustrate the over-selection and under-selection issues discussed earlier across a range of settings. These range from no confounding settings, where all covariates are instruments, to full confounding scenarios where all covariates are confounders. We also consider single and multiple treatments, as well as varying sample sizes and problem dimensions. We next present two separate case studies. Section 4.2 studies the association between certain demographics and the hourly salary, and its evolution between 2010 and 2019 (prior to COVID-19, to avoid potential pandemic-related distortions), to assess progress in wage discrimination. In Section 4.3 we analyse a putative association between less favorable environmental conditions at birth and subsequent crime levels some years later, following a study carried out by Donohue III and Levitt [2001], followed up by Belloni et al. [2014].

In Section 4.1 we compare our CIL (under the EP approximation) to DL based on the LASSO [Belloni et al., 2014], BAC [Wang et al., 2012], ACPME [Wilson et al., 2018], a standard LASSO regression on the outcome equation (1) (setting the penalization parameter via cross-validation), and standard BMA with a Beta-Binomial(1, 1) model prior and the pMOM prior on the coefficients (Section 2). We compare these methods to the oracle OLS, i.e. based on the subset of covariates truly featuring in (1). In Section 4.2 we focus on DL, standard BMA and, since n is large relative to the number of parameters, we also consider ordinary least-squares (OLS) under the full model. We did not include BAC and ACPME here, as they failed to return results after 2 days (ACPME also exhausted 96Gb of RAM memory). Finally, in Section 4.3 we consider DL, BAC, ACPME and standard BMA. These methods are implemented in R packages `glmnet` [Friedman et al., 2010] for the LASSO, `mombf` for BMA, `hdm` [Chernozhukov et al., 2016] for DL, `bacr` [Wang, 2016] for BAC and `regimes` [Wilson, 2023] for ACPME. Throughout we set the BAC hyper-parameter to $\omega = +\infty$, which is the default in R package `bac` and encourages the inclusion of confounders relative to standard BMA. R code to reproduce all our analyses is at https://github.com/mtorrens/cil_article.

4.1. Simulation Studies.

4.1.1. *Single treatment.* We consider an outcome generated according to (1) under a Gaussian likelihood, a single treatment ($T = 1$), and an error variance $\phi = 1$. The covariates are obtained as independent Gaussian draws $\mathbf{x}_j \sim N(\mathbf{0}, \mathbf{I})$, with any active covariate affecting y_i having an associated coefficient $\beta_j = 1$. The treatment d_i is generated to be a linear combination of the covariates, plus a zero-mean Gaussian random error with unit variance. Similarly to y_i , covariates having an effect on d_i have a unit regression coefficient. In all simulations, we set the total number of covariates that truly have an effect on d_i to be equal to $|\boldsymbol{\gamma}|_0$, the number of covariates that have an effect on the outcome y_i . To illustrate issues associated to under- and over-selection of covariates, a key factor we focus on is the *level of confounding*. Our scenarios range from no confounding (none of the $|\boldsymbol{\gamma}|_0$ covariates affecting y_i have an effect on d_i) to complete confounding (all $|\boldsymbol{\gamma}|_0$ covariates affecting y_i also affect d_i). We measure the square-root MSE (RMSE) of the estimated $\hat{\alpha}$.

Figure 1 summarizes the results when the number of active covariates is $|\boldsymbol{\gamma}|_0 = 6$ out of a total of $J = 49$, $n = 100$, and the treatment effect is either strong ($\alpha = 1$), weak ($\alpha = 1/3$), or non-existent ($\alpha = 0$). The two main features are as follows. First, standard high-dimensional methods such as LASSO and BMA incur a high RMSE in high-confounding settings, whereas methods such as DL and BAC

that are designed to prevent omitted variable biases perform much better in this regime. Second, in low confounding settings DL and BAC incur a high RMSE, due to the over-selection of instruments into the outcome equation. ACPME mimics the same RMSE pattern as these two, overshooting the model size less than BAC, but similarly to DL (see Figure 11). In contrast, our CIL performs well at all levels of confounding. Note also that, when there truly is no treatment effect, CIL (and BMA, in some instances) attains a much lower RMSE than the oracle OLS. This occurs because CIL effectively shrinks the treatment estimate to zero. Of course, it is possible to modify methods such as BAC or ACPME to also run selection on the treatment and one would then expect a comparable shrinkage, our results simply point out the potential benefits in conducting selection on the treatment effects. The Empirical Bayes and the Expectation Propagation versions of CIL provide nearly indistinguishable results (not shown).

Figure 11 complements these results by showing the average size of the selected outcome model (top panels), and the probability of selecting the treatment (bottom panels). The results indicate that, as expected, the RMSE inflation incurred by LASSO and BMA in high-confounding settings is due to omitted variable biases.

We next consider two extensions of our simulation study. First, Figure 12 considers a growing number of covariates, specifically $J + T = \{25, 100, 200\}$ with corresponding sample sizes $n = \{50, 100, 100\}$, in all cases under a strong treatment effect ($\alpha = 1$). As dimensionality grows, the standard LASSO and BMA incur a significantly higher RMSE under strong confounding. Our CIL generally provides a significantly lower RMSE over BMA in high-confounding scenarios, and a similar RMSE under mild and no confounding. An exception is the larger $J + T = 200$, where under mild and no confounding the RMSE for BMA was roughly half that for CIL, although the latter was still significantly better than DL and BAC. At $J + T = 100$, ACPME departs from the behavior pattern of BAC and sensibly improves its relative performance for low levels of confounding, although it cannot attain the results of CIL. At $J + T = 200$, where $n < J + T$, ACPME cannot be computed. It is in this latter setting where we observe the only perceptible differences between the EB and EP approximations, with the former attaining better results, pointing to advantages of the EB approach in higher dimensions.

As a second extension, Figure 13 shows the results when considering less sparse settings, specifically with $|\gamma|_0 = 6, 12$ and 18 active parameters. Overall, the results are similar to Figures 1 and 12. Our CIL continued to provide a competitive and more robust behavior across levels of confounding, relative to the other considered methods. It is worth noting that again ACPME is able to improve the results of BAC,

although it still cannot match the performance of CIL, particularly in low confounding scenarios.

4.1.2. Multiple treatments. To help understand under- and over-selection issues in multiple treatment inference, we consider an increasing number of treatments, with a maximum of $T = 5$. There, every present treatment is active, setting $\alpha_t = 1$ on all treatments. For all levels of T , we set $\beta_j = 1$ for $j = 1, \dots, 20$, denoting the set of active covariates by $\mathbf{x}_{1:20}$, and $\beta_j = 0$ for the rest of covariates $\mathbf{x}_{21:J}$. Regarding the association between treatments and covariates, $\mathbf{x}_{1:20}$ are divided into five disjoint subsets with four variables each, and each of these subsets is associated to a different treatment. The treatments depend linearly on the covariates of its associated subset. Additionally, each treatment also depends on a further subset of inactive covariates $\mathbf{x}_{21:J}$, i.e. instruments. In this case, the size of such subset is increasing by four with each added treatment: treatment 1 is associated to $\mathbf{x}_{21:24}$, treatment 2 is associated to $\mathbf{x}_{21:28}$, etc., up to treatment 5, which is associated to $\mathbf{x}_{21:40}$. All covariates affecting a treatment has a unit linear coefficient. The idea is that, as one considers a larger number of treatments T , one expects that potential ill-effects of over-selecting instruments and under-selecting confounders may become more problematic. Accordingly, as described our simulation considers $4T$ confounders and a growing number of instruments (4, 8, 12, 16, 20) for $T = (1, 2, 3, 4, 5)$. The rest of the design is as in Figure 1.

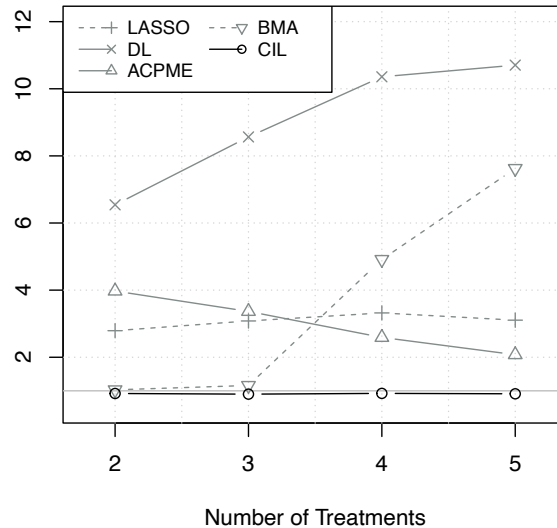


FIGURE 3. Treatment parameter RMSE (relative to oracle OLS) based on $R = 250$ simulated datasets at every value of T , for $n = 100$, $J = 95$, and $T \in \{2, 3, 4, 5\}$. For every T (x -axis), we show the average RMSE across Treatments $1, \dots, T$.

Figure 3 shows the RMSE associated to $\hat{\alpha}$ for the different values of T , i.e.

$$\text{RMSE}_T = \frac{1}{T} \sum_{t=1}^T \text{RMSE}(\hat{\alpha}_t, \alpha_t^*)$$

where α_t^* is the data-generating truth and $\hat{\alpha}_t$ the estimate provided by each method. We observe similar trends as before. Methods prone to over-selection recover more instruments as T increased. Some of these covariates are increasingly influential with T as they are associated to more treatments, and so they become harder to discard. Interestingly, ACPME was designed to ameliorate the over-selection of instruments in multiple treatment settings, and indeed we observe an improved behavior as T grows. Still, its RMSE ranged from 2 to 4 times larger than that of CIL.

It is also interesting to remark that under-selection issues (here suffered by BMA) are also problematic. As T grows the model becomes highly confounded, as a subset of the covariates account for a larger proportion of the variance in the outcome, as well as for that of the treatments. This leads to BMA discarding with high probability confounders that are truly active but are highly correlated to the treatments. Our CIL proposal is able to achieve oracle-type performance for every considered T .

4.2. Salary variation and discriminating factors. We analyze the USA Current Population Survey (CPS) microdata [Flood et al., 2020], which records many social, economic and job-related factors. We download data from 2010 and 2019 and analyze each year separately (see Section H.2 for details on data acquisition and pre-processing). We select individuals aged over 18, with a yearly income over \$1,000 and working 20-60 hours per week, giving $n = 64,380$ and $n = 58,885$ in 2010 and 2019, respectively. The covariates include characteristics of the place of residence, education, labor force status, migration status, household composition, housing type, health status, financial records, reception of subsidies, and sources of income (beyond wage). Overall, there are $J = 278$ covariates, 228 given in the raw data plus 50 indicators for state. The outcome is the individual log-hourly wage, rescaled by the consumer price index of 1999, and we consider $T = 4$ main treatments of interest: gender, black race, Hispanic ethnicity and Latin America as place of birth. These treatments are highly correlated to sociodemographic and job characteristics that can impact salary, i.e. there are many potential confounders. Since every state has its own regulatory, sociodemographic and political framework, we capture heterogeneous state effects by adding interactions for each pair of treatment and state. On these interactions, we apply a sum to zero constraint, so that the coefficients associated to the four treatments

remain interpretable as average treatment effects across the USA, and the interactions as deviation from the average. Hence, overall we have $4 + 4 \times 50 = 204$ parameters quantifying treatment effects, and our main interest is in the first four. To simplify computation in our CIL prior we assume a common θ_t shared between each main treatment and all its interactions with state, so that $\dim(\boldsymbol{\theta}) = 5$.

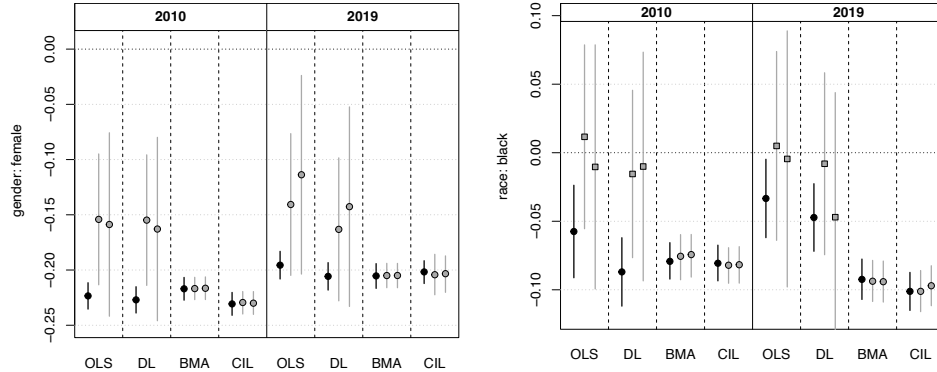


FIGURE 4. Inference for treatments “female” (left) and “black” (right) in 2010 and 2019. We analyze Current Population Survey data with $J = 278$ covariates (left black point and bar in each panel) but also adding 100 (middle) and 200 (right) artificial instruments. Names of methods as in the caption of Figure 1.

Figure 4 reports the results for gender and race. More detailed results in Figure 10 show that none of the methods finds an association between salary variation and ethnicity or place of birth. The treatment effect for gender is picked up by all methods in both years with similar point estimates. All methods suggest a slight decrease of this effect in 2019. For race the methods vary in their findings. All methods find a negative association between black race and salary, but in 2019 OLS and DL estimate a fairly lower effect.

In order to understand this difference better, and explore whether it is due to over-selection, we analyze two additional augmented datasets where we add artificial instruments. Specifically, we incorporate 100 instruments in the first scenario, and 200 in the second one. The instruments are split into four equal subsets, each of which is designed to correlate to one of the four main treatments, see Section H.3 for full details. The resulting average correlation between gender and its associated artificial instruments is 0.83, and analogously 0.69, 0.76 and 0.67 for black race, ethnicity and place of birth. Upon adding said instruments, the confidence intervals for OLS and DL become notably wider, whereas CIL and BMA results remain particularly robust. This

variance inflation is particularly pronounced for the effect of black race, which in 2019 lead to a loss of statistical significance according to OLS and DL. These findings suggest that the smaller racial gap estimated in 2019 in the original data may be due to variance inflation rather than an actual improvement in the racial gap.

The full scope of a Bayesian inferential framework is materialized when, additionally to quantifying treatment effects, one also considers more complex functions of the parameters. As an illustration, we study a measure of overall treatment contribution to deviations from the average salary. The idea is that the conditional associations between salary and the four treatments (gender, race, Hispanic ethnicity and birth in Latin America) may reflect salary discrimination associated to these demographics, and it is hence interesting to quantify the overall effect of all four treatments. For a new observation $n + 1$, with observed treatments \mathbf{d}_{n+1} and covariates \mathbf{x}_{n+1} , let

$$\begin{aligned} h_{n+1}(\mathbf{d}_{n+1}, \boldsymbol{\alpha}, \mathbf{x}_{n+1}) &= |\mathbb{E}(y_{n+1} \mid \mathbf{d}_{n+1}, \mathbf{x}_{n+1}, \boldsymbol{\alpha}, \boldsymbol{\beta}) - \mathbb{E}(y_{n+1} \mid \mathbf{x}_{n+1}, \boldsymbol{\alpha}, \boldsymbol{\beta})| \\ (15) \quad &= |[\mathbf{d}_{n+1} - \mathbb{E}(\mathbf{d}_{n+1} \mid \mathbf{x}_{n+1})]^\top \boldsymbol{\alpha}| \end{aligned}$$

be its expected salary minus the expected salary averaged over possible \mathbf{d}_{n+1} , given equal covariate values \mathbf{x}_{n+1} . Since y_{n+1} is a log-salary, we examine the posterior predictive distribution of $\exp \{h_{n+1}(\mathbf{d}_{n+1}, \boldsymbol{\alpha}, \mathbf{x}_{n+1})\}$ as a measure of salary variation associated to the treatments. A value of 1 indicates no deviation from the average salary, relative to another individual with the same covariates \mathbf{x}_{n+1} .

To evaluate the posterior predictive distribution of (15) given \mathbf{y} , the observed \mathbf{d} and the set of covariates, we obtain posterior samples from the model averaged posterior $p(\boldsymbol{\alpha} \mid \mathbf{y})$ associated to CIL (Section 3.1). Given that we do not have an explicit model for $(\mathbf{d}_{n+1}, \mathbf{x}_{n+1})$, we sample pairs $(\mathbf{d}_{n+1}, \mathbf{x}_{n+1})$ from their empirical distribution, and estimate $\mathbb{E}(\mathbf{d}_{n+1} \mid \mathbf{x}_{n+1})$ from a logistic regression of \mathbf{d} on the set of covariates. Figure 5 shows the results. There is fairly little progress in reducing the joint association between the outcome and treatments, i.e. the potentially discriminatory factors, both at nation- and state-wide level (upper and lower panels in Figure 5, respectively). In 2010, joint variation in the treatments is associated to an average 6.2% salary variation (90% predictive interval [0.2%, 19.8%]). The posterior mean in 2019 drops slightly to 5.9% and the 90% predictive interval is [0.2%, 17.8%]. That is, the treatments play a similar role in the 2019 both in average and in the whole predictive distribution.

It is also of interest to study differences between states. This is possible in our model, which features 200 interaction terms for the 4 treatments and 50 states. Figure 5 (right) shows the results. The most salient feature is a slightly lower heterogeneity across states in 2019 relative to 2010. The three states whose median improves the most are

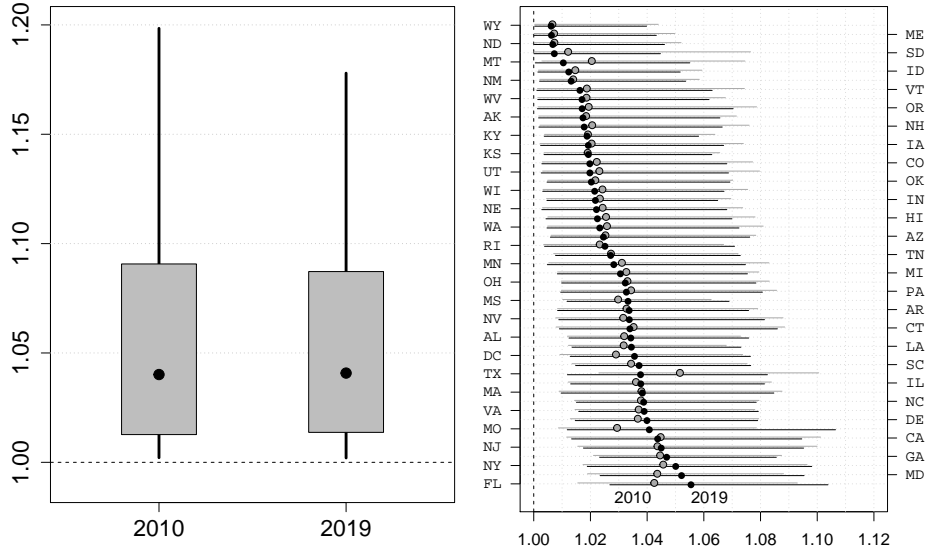


FIGURE 5. The left panel shows the posterior predictive distribution of deviations from average salary as given by $\exp\{h_{n+1}(\mathbf{d}_{n+1}, \boldsymbol{\alpha}, \mathbf{x}_{n+1})\}$ in (15), for 2010 and 2019. The gray boxes represent 50% posterior intervals and the black lines are 90% intervals. The black dot is the posterior median. The right panel shows the posterior median of these deviations for every U.S. state in 2010 and 2019 on the horizontal axis, ordered by their value in 2019, with the corresponding 50% posterior intervals for both years.

Texas (reducing it by 1.4%), Montana (1.0%) and South Dakota (0.5%), while the three in which it worsens the most are Florida (increasing it by 1.3%), Missouri (1.1%) and Maryland (0.9%), which are already among the bottom-ranking states in 2010.

4.3. Abortion and Crime Study. Belloni et al. [2014] revisit a study by Donohue III and Levitt [2001] that assesses the association between yearly state-level abortion rates and crime rates 15–25 years later. A hypothesis is that, if parents choose a moment of birth to raise children in a favorable environment, the latter might be less likely to commit crimes when they reach ages 15–25. The authors consider three crime types (violent, property, murder) and a measure of abortion associated to each type (a weighted average of abortion rates across age groups, where the weights are the fraction of that crime type committed by each age group).

To avoid confounding when estimating the association between abortion and crime, it is important to account for state and time effects for the period 1985 to 1997, and various other covariates. Donohue III and Levitt [2001] consider the log of prisoners per capita and of police per

TABLE 1. Estimated association between three crime types and abortion

	Violent crime			
	Estimate	95% interval	<i>p</i> -value	$P(\alpha \neq 0 \mid \mathbf{y})$
Donohue III and Levitt	-0.13	(-0.18, -0.08)	< 0.001	—
OLS (all covariates)	-0.04	(-1.37, 1.30)	0.958	—
DL	-0.21	(-0.46, 0.04)	0.105	—
BAC	0.37	(-0.67, 1.28)	—	—
ACPME	-0.42	(-0.54, -0.31)	—	—
BMA (Normal)	-0.07	(-0.29, 0)	—	0.216
BMA (MOM)	-0.01	(-0.16, 0)	—	0.032
CIL (Normal)	-0.17	(-0.31, 0)	—	0.977
CIL (MOM)	-0.11	(-0.24, 0)	—	0.657
Property crime				
Donohue III and Levitt	-0.90	(-0.94, -0.87)	< 0.001	—
OLS (all covariates)	-0.19	(-0.56, 0.19)	0.327	—
DL	-0.04	(-0.12, 0.04)	0.369	—
BAC	-0.16	(-0.42, 0.11)	—	—
ACPME	-0.14	(-0.22, -0.07)	—	—
BMA (Normal)	0	(0, 0)	—	0.063
BMA (MOM)	0.00	(0, 0)	—	0.001
CIL (Normal)	-0.05	(-0.15, 0)	—	0.593
CIL (MOM)	-0.02	(-0.12, 0)	—	0.122
Murder				
Donohue III and Levitt	-0.12	(-0.21, -0.03)	0.010	—
OLS (all covariates)	1.73	(-3.70, 7.15)	0.531	—
DL	-0.12	(-0.95, 0.716)	0.785	—
BAC	-0.25	(-3.47, 3.01)	—	—
ACPME	-0.51	(-0.91, -0.11)	—	—
BMA (Normal)	0	(0, 0)	—	0.009
BMA (MOM)	0	(0, 0)	—	< 0.001
CIL (Normal)	-0.03	(-0.61, 0.10)	—	0.136
CIL (MOM)	0	(0, 0)	—	0.003

capita, unemployment and poverty rates, income and beer consumption per capita, the aid to families with dependent children (AFDC) program generosity, the existence of a concealed guns law, and the one-year lagged versions of these variables. Belloni et al. [2014] extend the analysis by adding quadratic covariate effects, interactions and linear and quadratic interactions with time. To account for state effects, they define the response as the increase in crime rates between two consecutive years, the treatment as the increase in abortion rates, and they include as covariates the within-state crime averages and the initial crime rates at 1985. They also force the inclusion of the year indicators

in the model to avoid their estimates being driven by time dynamics in crime and abortion. The additions of Belloni et al. [2014] are done to reduce the misspecification of the outcome model, which could hamper causal interpretations. Our analysis keeps these covariates and overall we have $n = 576$ observations, 1 treatment and $J = 295$ covariates. Further details are provided in Section H.5.

Table 1 summarizes the results obtained with different approaches, the previous ones and the one we develop in this article. The least-squares analysis of Donohue III and Levitt [2001] based on a pre-defined set of covariates find a statistically significant association between abortion and the three crime types. For comparison we also run a least-squares regression using all covariates considered by Belloni et al. [2014], which returns no statistically significant results and very wide confidence intervals. This is as expected in situations where covariates are strongly correlated with the treatment. The DL analysis of Belloni et al. [2014] also returns no statistically significant associations, which we update here using the latest version (0.3.1) of their R package `hdm`. The main difference between DL and Donohue III and Levitt [2001] is that the former selected numerous covariates that are associated to the treatment (abortion) but not to the outcome, i.e. likely instruments. For violent crime, a LASSO analysis of the outcome equation selected no covariates, whereas 9 covariates are selected in the abortion equation. DL then proceeded by regressing violent crime on those 9 covariates. As shown in Table 1, adding said covariates that are highly correlated with abortion causes a variance inflation in the estimated effect for the latter. Also note that there is little evidence that the covariates are needed in the outcome equation, e.g. only one of their naive p -values (not accounting for post-selection inference) are below 0.05 (Table S1). A similar situation occurs for property crime and murder. For property crime 13 covariates are selected (1 p -value below 0.05), and for murder it is 8 covariates (no p -value below 0.05). Applying BAC to these data gives qualitatively similar results to DL, in that no significant treatment effect is detected. Again a potential issue is that many covariates have a non-negligible contribution, which can cause variance inflation, e.g. 98 covariates have marginal posterior inclusion probability above 0.5 for violent crime, 97 for property crime, and 80 for murder. ACPME did find a significant association for all three crime types. This is interesting because, as discussed, ACPME presents similarities to BAC but attempts to ameliorate variance inflation due to selecting instruments.

We re-analyze the data of Belloni et al. [2014] with standard BMA (Beta-Binomial model prior) and our CIL methodology, also forcing the inclusion of the year indicators in the model, following Belloni et al. [2014]. To explore sensitivity of the results to the prior, we obtain results under a default normal prior on the parameters with

diagonal covariance and a MOM prior with default dispersion. As shown in Table 1, the results of our CIL approach lie somewhere in between the significant results found by Donohue III and Levitt [2001] and by ACPME, and the non-significant results found by DL, BAC and BMA. In the violent crime analysis, CIL finds moderate evidence for a negative association between abortion and crime. Under CIL all covariates have a negligible posterior inclusion probability. This is contrast to BMA where several covariates (6 for BMA normal, 2 for BMA MOM) have posterior inclusion probabilities above 0.1, and to DL which selects 8 covariates (which, as discussed, are likely to be instruments). We observe a similar situation for property crime, where CIL produces higher posterior probabilities for the existence of an association than its BMA counterpart. However, these are only moderate and the estimated effect is small. For murder CIL finds no evidence for an association with abortion. See Section H.5 for a discussion on the covariates selected by BMA and CIL in each analysis.

Overall the CIL results provide moderate, but not overwhelming, evidence for the existence of an association between abortion and crime (violent crime in particular). On the basis of CIL’s analysis the applied researcher might try and obtain further evidence to evaluate the assumed association, whereas the results with DL and BMA could be construed as fairly strong evidence against said association.

5. DISCUSSION

The two main ingredients in our proposal are learning from data whether and to what extent covariate inclusion/exclusion should be encouraged to improve multiple treatment inference, and a convenient computational strategy to render the approach practical. By learning the relative importance of potential confounders one hopes to obtain a better balance between over-selection of instruments and under-selection of confounders.

These issues are practically relevant, e.g. in the salary data we show that one may underestimate the association black race and salary. Further, the proposed Bayesian framework naturally allows for posterior predictive inference on functions that depend on multiple parameters, such as the variation in salary jointly associated with multiple treatments. Interestingly, our analyses reveal little progress in the association between salary and potentially discriminatory factors such as gender or race in 2019 relative to 2010, nation- and state-wise. These results are conditional on covariates that include education, employment and other characteristics that affect salary. That is, our results reveal lower salary discrepancies in 2019 between races/genders, provided that two individuals have the same characteristics (and that they were hired in the first place). This analysis offers a complementary view to analyses that are unadjusted by confounders, and which may reveal

equally interesting information. For example, if females migrated towards lower-paying occupational sections in 2019 and received a lower salary as a consequence, this would not be detected by our analysis, but would be revealed by an unadjusted analysis.

We remark that our methodology can be extended to other settings where one wishes to treat the inclusion of covariates non-exchangeably a priori. For example, an interesting avenue for future research are settings where one has meta-covariates distinguishing covariate subsets (e.g. clinical variables, genomic markers, diagnostic tests), where it is natural to consider that different subsets may warrant different inclusion probabilities.

6. ACKNOWLEDGMENTS

David Rossell gratefully acknowledges support from grant *Consolidación investigadora* CNS2022-135963 by the AEI (Government of Spain), *Ayudas Fundación BBVA Proyectos de Investigación Científica en Matemáticas 2021*, Huawei research grants, Europa Excelencia EUR2020-112096 from the AEI/10.13039/501100011033 and European Union NextGenerationEU/PRT, and grant PID2022-138268NB-I00 financed by MCIN/AEI/10.13039/501100011033 and the FSE+.

APPENDIX A. PROOF OF PROPOSITION 3.1

The empirical Bayes estimate writes

$$\boldsymbol{\theta}^{\text{EB}} = \arg \max_{\boldsymbol{\theta} \in \mathbb{R}^{T+1}} \log p(\mathbf{y} \mid \boldsymbol{\theta}) = \arg \max_{\boldsymbol{\theta} \in \mathbb{R}^{T+1}} \log \sum_{(\boldsymbol{\gamma}, \boldsymbol{\delta})} p(\mathbf{y} \mid \boldsymbol{\gamma}, \boldsymbol{\delta}) p(\boldsymbol{\gamma}, \boldsymbol{\delta} \mid \boldsymbol{\theta}).$$

For short, denote $H(\boldsymbol{\theta}) = p(\mathbf{y} \mid \boldsymbol{\theta})$ and $h_j(\boldsymbol{\theta}) = p_j(\gamma_j \mid \boldsymbol{\theta})$, where generically $\nabla_{\boldsymbol{\theta}} \log H(\boldsymbol{\theta}) = \nabla_{\boldsymbol{\theta}} H(\boldsymbol{\theta})/H(\boldsymbol{\theta})$. Under the assumptions of Proposition 3.1

$$\begin{aligned} \nabla_{\boldsymbol{\theta}} H(\boldsymbol{\theta}) &= \sum_{(\boldsymbol{\gamma}, \boldsymbol{\delta})} p(\mathbf{y} \mid \boldsymbol{\gamma}, \boldsymbol{\delta}) p(\boldsymbol{\delta}) \nabla_{\boldsymbol{\theta}} \prod_{j=1}^J h_j(\boldsymbol{\theta}) \\ (16) \quad &= \sum_{(\boldsymbol{\gamma}, \boldsymbol{\delta})} p(\mathbf{y} \mid \boldsymbol{\gamma}, \boldsymbol{\delta}) p(\boldsymbol{\delta}) \sum_{j=1}^J \left(\nabla_{\boldsymbol{\theta}} h_j(\boldsymbol{\theta}) \prod_{l \neq j} h_l(\boldsymbol{\theta}) \right). \end{aligned}$$

Denoting $\mathbf{f}_j = (1, f_{j,1}, \dots, f_{j,T})^\top$, direct algebra gives

$$(17) \quad \nabla_{\boldsymbol{\theta}} h_j(\boldsymbol{\theta}) = (1 - 2\rho) \mathbf{f}_j (\gamma_j - \pi_j(\boldsymbol{\theta})) h_j(\boldsymbol{\theta}).$$

Then, replacing (17) into (16)

$$\begin{aligned}
 \nabla_{\boldsymbol{\theta}} H(\boldsymbol{\theta}) &= \sum_{(\boldsymbol{\gamma}, \boldsymbol{\delta})} p(\mathbf{y} \mid \boldsymbol{\gamma}, \boldsymbol{\delta}) p(\boldsymbol{\delta}) \sum_{j=1}^J (1 - 2\rho) \mathbf{f}_j (\gamma_j - \pi_j(\boldsymbol{\theta})) \prod_{l=1}^J h_l(\boldsymbol{\theta}) \\
 &= \sum_{j=1}^J (1 - 2\rho) \mathbf{f}_j \sum_{(\boldsymbol{\gamma}, \boldsymbol{\delta})} (\gamma_j - \pi_j(\boldsymbol{\theta})) p(\mathbf{y} \mid \boldsymbol{\gamma}, \boldsymbol{\delta}) p(\boldsymbol{\delta}, \boldsymbol{\gamma} \mid \boldsymbol{\theta}) \\
 &= \sum_{j=1}^J (1 - 2\rho) \mathbf{f}_j \left[(1 - \pi_j(\boldsymbol{\theta})) \sum_{(\boldsymbol{\gamma}, \boldsymbol{\delta}): \gamma_j=1} p(\mathbf{y}, \boldsymbol{\delta}, \boldsymbol{\gamma} \mid \boldsymbol{\theta}) - \pi_j(\boldsymbol{\theta}) \sum_{(\boldsymbol{\gamma}, \boldsymbol{\delta}): \gamma_j=0} p(\mathbf{y}, \boldsymbol{\delta}, \boldsymbol{\gamma} \mid \boldsymbol{\theta}) \right].
 \end{aligned}$$

Finally

$$\begin{aligned}
 \nabla_{\boldsymbol{\theta}} \log H(\boldsymbol{\theta}) &= \frac{\nabla_{\boldsymbol{\theta}} H(\boldsymbol{\theta})}{H(\boldsymbol{\theta})} = \\
 &= \sum_{j=1}^J (1 - 2\rho) \mathbf{f}_j \left[(1 - \pi_j(\boldsymbol{\theta})) \frac{\sum_{(\boldsymbol{\gamma}, \boldsymbol{\delta}): \gamma_j=1} p(\mathbf{y}, \boldsymbol{\delta}, \boldsymbol{\gamma} \mid \boldsymbol{\theta})}{\sum_{(\boldsymbol{\gamma}, \boldsymbol{\delta})} p(\mathbf{y}, \boldsymbol{\delta}, \boldsymbol{\gamma} \mid \boldsymbol{\theta})} - \pi_j(\boldsymbol{\theta}) \frac{\sum_{(\boldsymbol{\gamma}, \boldsymbol{\delta}): \gamma_j=0} p(\mathbf{y}, \boldsymbol{\delta}, \boldsymbol{\gamma} \mid \boldsymbol{\theta})}{\sum_{(\boldsymbol{\gamma}, \boldsymbol{\delta})} p(\mathbf{y}, \boldsymbol{\delta}, \boldsymbol{\gamma} \mid \boldsymbol{\theta})} \right] \\
 &= \sum_{j=1}^J (1 - 2\rho) \mathbf{f}_j [(1 - \pi_j(\boldsymbol{\theta})) P(\gamma_j = 1 \mid \mathbf{y}, \boldsymbol{\theta}) - \pi_j(\boldsymbol{\theta}) (1 - P(\gamma_j = 1 \mid \mathbf{y}, \boldsymbol{\theta}))] \\
 &= (1 - 2\rho) \sum_{j=1}^J \mathbf{f}_j [P(\gamma_j = 1 \mid \mathbf{y}, \boldsymbol{\theta}) - \pi_j(\boldsymbol{\theta})].
 \end{aligned}$$

■

APPENDIX B. PROOF OF PROPOSITION 3.2

Consider the optima of the marginal likelihood,

$$(18) \quad \arg \max_{\boldsymbol{\theta} \in \mathbb{R}^{T+1}} \sum_{(\boldsymbol{\delta}, \boldsymbol{\gamma})} p_0(\boldsymbol{\delta}, \boldsymbol{\gamma} \mid \mathbf{y}) p(\boldsymbol{\delta}, \boldsymbol{\gamma} \mid \boldsymbol{\theta})$$

where $p_0(\boldsymbol{\delta}, \boldsymbol{\gamma} \mid \mathbf{y})$ are the posterior probabilities under a uniform prior $p_0(\boldsymbol{\delta}, \boldsymbol{\gamma}) \propto 1$. We seek to set the parameters s_t and r_j in the approximation

$$q(\boldsymbol{\delta}, \boldsymbol{\gamma} \mid \mathbf{y}) = \prod_{t=1}^T \text{Bern}(\delta_t; s_t) \prod_{j=1}^J \text{Bern}(\gamma_j; r_j)$$

using Expectation Propagation. That is, setting and $\mathbf{r} = (r_1, \dots, r_J)$ such that

$$\mathbf{r}^{\text{EP}} = \arg \max_{\mathbf{r} \in [0, 1]^J} \sum_{(\boldsymbol{\gamma}, \boldsymbol{\delta})} p_0(\boldsymbol{\delta}, \boldsymbol{\gamma} \mid \mathbf{y}) \log \left(\prod_{t=1}^T s_t^{\delta_t} (1 - s_t)^{1 - \delta_t} \prod_{j=1}^J r_j^{\gamma_j} (1 - r_j)^{1 - \gamma_j} \right).$$

and analogously for $\mathbf{s} = (s_1, \dots, s_T)$. Proceeding elementwise, we derive

$$\begin{aligned}
 r_j^{\text{EP}} &:= \arg \max_{r_j \in [0,1]} \sum_{(\boldsymbol{\gamma}, \boldsymbol{\delta})} p_0(\boldsymbol{\delta}, \boldsymbol{\gamma} \mid \mathbf{y}) \times \\
 &\left(\sum_{j=1}^J [\gamma_j \log r_j + (1 - \gamma_j) \log(1 - r_j)] + \sum_{t=1}^T [\delta_t \log s_j + (1 - \delta_t) \log(1 - s_t)] \right) \\
 &= \arg \max_{r_j \in [0,1]} \sum_{(\boldsymbol{\gamma}, \boldsymbol{\delta})} p_0(\boldsymbol{\delta}, \boldsymbol{\gamma} \mid \mathbf{y}) \left[\sum_{j=1}^J [\gamma_j \log r_j + (1 - \gamma_j) \log(1 - r_j)] \right] \\
 &= \arg \max_{r_j \in [0,1]} \sum_{j=1}^J \sum_{(\boldsymbol{\gamma}, \boldsymbol{\delta})} p_0(\boldsymbol{\delta}, \boldsymbol{\gamma} \mid \mathbf{y}) [\gamma_j \log r_j + (1 - \gamma_j) \log(1 - r_j)].
 \end{aligned}$$

Optimizing this expression yields

$$\begin{aligned}
 \frac{\partial}{\partial r_j} &= 0 \Leftrightarrow \sum_{(\boldsymbol{\gamma}, \boldsymbol{\delta})} p_0(\boldsymbol{\delta}, \boldsymbol{\gamma} \mid \mathbf{y}) \left(\frac{\gamma_j}{r_j^{\text{EP}}} - \frac{1 - \gamma_j}{1 - r_j^{\text{EP}}} \right) = 0 \\
 \Leftrightarrow \frac{1}{r_j^{\text{EP}}} &\sum_{(\boldsymbol{\gamma}, \boldsymbol{\delta}): \gamma_j=1} p_0(\boldsymbol{\delta}, \boldsymbol{\gamma} \mid \mathbf{y}) - \frac{1}{1 - r_j^{\text{EP}}} \sum_{(\boldsymbol{\gamma}, \boldsymbol{\delta}): \gamma_j=0} p_0(\boldsymbol{\delta}, \boldsymbol{\gamma} \mid \mathbf{y}) = 0 \\
 \Leftrightarrow \frac{P_0(\gamma_j = 1 \mid \mathbf{y})}{r_j^{\text{EP}}} &- \frac{P_0(\gamma_j = 0 \mid \mathbf{y})}{1 - r_j^{\text{EP}}} = 0 \\
 (19) \Leftrightarrow r_j^{\text{EP}} &= P_0(\gamma_j = 1 \mid \mathbf{y}) = P(\gamma_j = 1 \mid \mathbf{y}, \boldsymbol{\theta} = \mathbf{0}).
 \end{aligned}$$

With the same exact procedure one analogously obtains $s_t^{\text{EP}} = P_0(\delta_t = 1 \mid \mathbf{y})$. ■

APPENDIX C. SUPPLEMENTARY MATERIAL

APPENDIX D. OVER-SELECTION BIAS

D.1. Discussion. As explained in the main text, selecting variables that are truly not associated to the outcome can introduce a bias in the estimated treatment effect. We remark that the issue does not occur when the selected variables are pre-specified, for example it's immediate to show that the least-squares estimator is unbiased for any model containing the truly active covariates plus a pre-defined set of extra covariates. The over-selection bias issue arises when variables are selected in a data-based fashion.

To illustrate this point we use two examples where there truly is no confounding. Consider a data-generating truth as in (1) where there is one treatment, $T = 1$, and the generative model for the covariates and the treatment is as follows: $\mathbf{x}_i \sim N(\mathbf{0}, \mathbf{I})$, $d_i \mid \mathbf{x}_i \sim N(\mathbf{x}_i^\top \mathbf{v}, 1)$, where unknown to the data analyst β has 3 non-zero entries and \mathbf{v} has 3 different non-zero entries, all equal to 2. Figure 6 (left) shows that the DL-based $\hat{\alpha}$ has a bias that grows with α and J and decreases with n (Belloni et al. [2014] showed that the bias vanishes as $n \rightarrow \infty$, under suitable conditions). The issue arises because the selection of covariates depends on the observed outcome. To obtain further insight, the right panel considers a setting where covariate selection is also outcome-dependent, in a simpler fashion. All entries in β and \mathbf{v} are truly 0, the analyst selects the covariate with the highest absolute correlation with the y_i 's and estimates α by OLS on the d_i 's and the selected covariate. The resultant estimate of α has a negative bias, which an analysis we carry out in the Supporting material approximates it to be

$$-c \frac{\alpha \phi}{\alpha^2 + \phi} \frac{\log J}{n},$$

for some constant $c > 0$. The simulation experiment in Figure 6 provides strong numerical evidence towards this approximation. This over-selection bias is fairly subtle, notice that both small and large signal-to-noise ratios $\alpha/\sqrt{\phi}$ lead to small bias but intermediate ones to large. In our experience said bias has little impact in most examples, unless J is really large relative to n . The take-home message is that, whereas for $J < n$ one may add all covariates to the model to obtain a (high-variance) unbiased estimator, when $J > n$ and one applies some shrinkage or selection, inference can be subject to bias.

The resultant over-selection mean squared error worsens as the number of treatments increases and as the the proportion of covariates that are relevant both for the response and the treatments decreases.

D.2. Derivations. We sketch an argument that is based on some explicit mathematical derivations, some careful numerics and educated guesses (based on intuitions from properties of maxima of Gaussians)

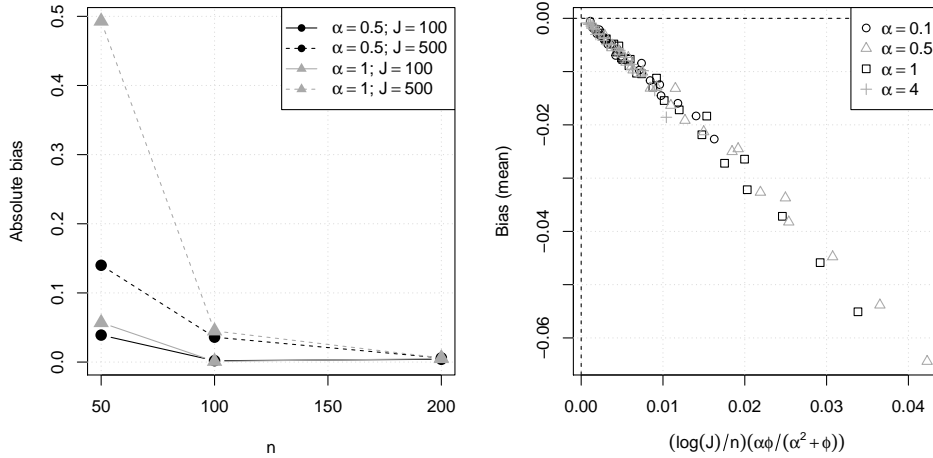


FIGURE 6. Over-selection bias simulations. The generative model for y_i is as in (1) with a Gaussian density, $\mathbf{x}_i \sim \mathcal{N}(\mathbf{0}, \mathbf{I})$ and $d_i \mid \mathbf{x}_i \sim \mathcal{N}(\mathbf{x}_i^\top \mathbf{v}, 1)$. Left: only three elements of $\boldsymbol{\beta}$ and three different ones of \mathbf{v} are non-zero, and all equal to 2, which makes the y_i 's indirectly correlated to three covariates whose corresponding elements in $\boldsymbol{\beta}$ are equal to zero. Said correlation becomes stronger as $|\alpha|$ grows. At the same time, screening out these covariates becomes harder as J/n increases, difficulting post-selection inference. Here $\hat{\alpha}$ is estimated with double-lasso, and we report absolute bias over 200 independent simulations for every condition. Right: $\boldsymbol{\beta}$ and \mathbf{v} are zero-vectors, the Gaussian observation variance is 0.5^2 , $\hat{\alpha}$ is estimated from OLS of y_i 's on d_i 's and the covariate selected among J available ones to have the highest correlation in absolute value with the y_i 's; the estimation is carried out for different $J \in \{10, 20, 40, 80, 160\}$ and $n \in \{30, 50, 100, 150, 200\}$ and the figure plots the estimated bias (over 15×10^3 independent experiments) versus $(\alpha \phi \log J)/(n(\alpha^2 + \phi))$, for $\phi = 0.5^2$, which is the approximation of the size of the bias suggested by the argument we develop in the Supporting material. Different colours correspond to different values of $\alpha \in \{1, 0.1, 0.5, 4\}$.

and quantifies the over-selection bias in a simple yet instructive example. As one can see from the following analysis, even in this simplified case it is not straightforward to obtain clean results, therefore we see this example as one that strikes a good balance between making an interesting point and being sufficiently tractable.

The setting is as follows. The data generating process is $\mathbf{y} \mid \mathbf{d} \sim \mathcal{N}(\alpha \mathbf{d}, \phi)$ where \mathbf{d} is random with mean 0 and variance 1. The analyst

has further available covariates \mathbf{x}_j that have been centered and scaled and unknown to them are independent of each other and \mathbf{d} and \mathbf{y} . Let

$$S = \arg \max_{1 \leq j \leq J} \mathbf{x}_j^\top \mathbf{y}$$

where, obviously, due to our setting S is marginally a uniformly distributed integer from 1 to J . (In the numerical experiment reported in Figure 6 we screen the predictor using $|\mathbf{x}_j^\top \mathbf{y}|$ but for the analysis here we omit the absolute value to simplify the problem. There are good reasons why this does not change the obtained result materially, which is why Figure 6 is in agreement with the result obtained using the analysis below). Let $\hat{\alpha}_S$ be the OLS estimate of α by regressing \mathbf{y} on \mathbf{d} and \mathbf{x}_S (without intercept). Application of standard OLS results show that $\hat{\alpha}_S = \alpha + \xi_S$ where

$$\xi_S = \frac{\mathbf{d}^\top (\mathbf{I} - \mathbf{x}_S \mathbf{x}_S^\top / n) (\mathbf{y} - \alpha \mathbf{d})}{\mathbf{d}^\top (\mathbf{I} - \mathbf{x}_S \mathbf{x}_S^\top / n) \mathbf{d}}.$$

We take $\mathbf{e} = (\mathbf{y} - \alpha \mathbf{d}) / \sqrt{\phi}$, which by construction has a standard Gaussian distribution. Direct calculation gives further that

$$\xi_S = \frac{\sqrt{\phi} \frac{\mathbf{d}^\top \mathbf{e}}{n}}{1 - (\mathbf{d}^\top \mathbf{x}_S / n)^2} - \frac{\sqrt{\phi}}{n} \frac{\frac{\mathbf{d}^\top \mathbf{x}_S}{\sqrt{n}} \frac{\mathbf{e}^\top \mathbf{x}_S}{\sqrt{n}}}{1 - \frac{1}{n} (\mathbf{d}^\top \mathbf{x}_S / \sqrt{n})^2}.$$

The first term is fairly symmetric around 0. We concentrate on the second term, and in particular the expectation of its numerator which will determine the bias, if any, to the highest order.

Notice that $\mathbf{x}_j^\top \mathbf{y} = \alpha \mathbf{x}_j^\top \mathbf{d} + \sqrt{\phi} \mathbf{x}_j^\top \mathbf{e}$, where $\mathbf{x}_j^\top \mathbf{d}$ and $\mathbf{x}_j^\top \mathbf{e}$ are uncorrelated, zero mean and have variance n . Hence, for obtaining an estimate of the bias we concentrate now on the simplified problem of approximating $\mathbb{E}[\gamma_S \delta_S]$ for

$$S = \arg \max_{1 \leq j \leq J} \left(\frac{\alpha}{\sqrt{\phi}} \gamma_j + \delta_j \right)$$

for γ_j, δ_j are i.i.d standard Gaussian. A basic exchangeability argument shows that for given J , as a function of r , when $S = \arg \max_j (r \gamma_j + \delta_j)$, $\mathbb{E}[\gamma_S \delta_S] = h(r)$ where $h(r) = h(1/r)$ and it is maximized at $r = 1$; such a function is $h(r) = 1/(r + 1/r)$. The intuition behind this result is that for very large or very small values of the ratio one of the two terms dominates the choice of S and the other is independent of that choice. An educated guess which builds upon results for maxima of Gaussian sequences is that to the highest order

$$\mathbb{E}[\gamma_S \delta_S] \approx c \frac{1}{r + 1/r} \log J$$

for some constant c (that does not depend on p or J). The results in Figure 7 provide strong numerical support for this conjecture.

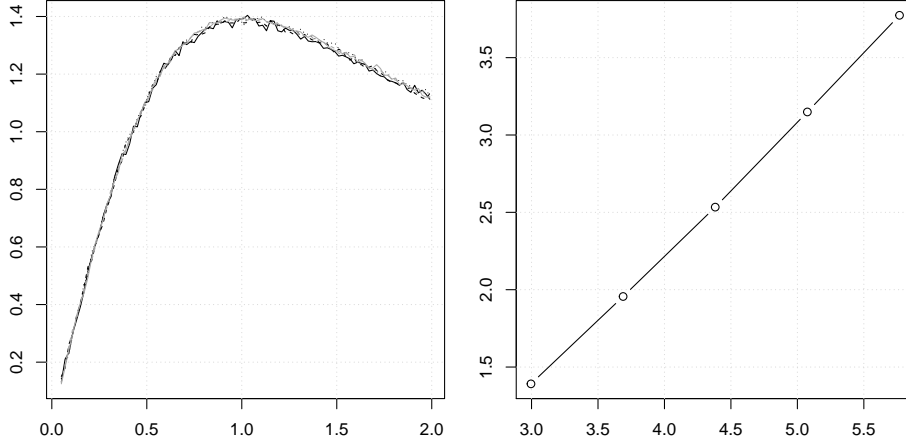


FIGURE 7. We show results of a large simulation study where we estimate $E[\gamma_S \delta_S]$, for $S = \arg \max_j (r\gamma_j + \delta_j)$ and γ_j, δ_j are i.i.d. standard Gaussian, for various values of J and r . On the left plot the estimates against the values of r , for the different values of J shown with different combinations of line type and color. We have scaled the curves to have the same value at $r = 1$ and the figure confirms the conjecture that the curves are the same up to multiplication of a function of J alone. On the right we plot the estimates that correspond to $r = 1$ against $\log J$ for the different values of J .

Putting all the steps together, we obtain an approximation of the bias to be

$$-c \frac{\alpha \phi}{\alpha^2 + \phi} \frac{\log J}{n}.$$

APPENDIX E. DERIVATIONS

E.1. **Derivation of Equation (14).** Let

$$h(\boldsymbol{\delta}) := \prod_{t=1}^T [s_t^{\text{EP}} \pi_t]^{\delta_t} [(1 - s_t^{\text{EP}})(1 - \pi_t)]^{1 - \delta_t},$$

which is independent of $\boldsymbol{\theta}$, and where π_t is the marginal prior inclusion probability within our framework. Then, implementing the approximation (19) into (18) gives

$$(20) \quad \boldsymbol{\theta}^{\text{EP}} := \arg \max_{\boldsymbol{\theta} \in \mathbb{R}^{T+1}} \sum_{(\boldsymbol{\gamma}, \boldsymbol{\delta})} h(\boldsymbol{\delta}) \times \prod_{j=1}^J [r_j^{\text{EP}} \pi_j(\boldsymbol{\theta})]^{\gamma_j} [(1 - r_j^{\text{EP}})(1 - \pi_j(\boldsymbol{\theta}))]^{1 - \gamma_j}.$$

Note that the product in the RHS of (20) defines a probability distribution on $(\delta_1, \dots, \delta_T, \gamma_1, \dots, \gamma_J)$ with independent components, hence the sum is the normalizing constant of such distribution. Thus, this constant is just the product of the univariate normalizing constants. The univariate normalizing constant of each Bernoulli is then

$$r_j^{\text{EP}} \pi_j(\boldsymbol{\theta}) + (1 - r_j^{\text{EP}})(1 - \pi_j(\boldsymbol{\theta}))$$

for every r_j , and similarly $s_t^{\text{EP}} \pi_t + (1 - s_t^{\text{EP}})(1 - \pi_t)$ for every s_t . Hence, replacing into (20) we directly obtain

$$(21) \quad \boldsymbol{\theta}^{\text{EP}} := \arg \max_{\boldsymbol{\theta} \in \mathbb{R}^{T+1}} \sum_{j=1}^J \log (r_j^{\text{EP}} \pi_j(\boldsymbol{\theta}) + (1 - r_j^{\text{EP}})(1 - \pi_j(\boldsymbol{\theta}))).$$

■

E.2. Gradient of Equation (14). Denote $h_j(\boldsymbol{\theta}) := r_j \pi_j(\boldsymbol{\theta}) + (1 - r_j)(1 - \pi_j(\boldsymbol{\theta}))$ for short. Simple algebra provides

$$\nabla_{\boldsymbol{\theta}} h_j(\boldsymbol{\theta}) = (2r_j - 1) \nabla_{\boldsymbol{\theta}} \pi_j(\boldsymbol{\theta}).$$

From (17) we recover the remaining gradient in the last expression and derive

$$\begin{aligned} \nabla_{\boldsymbol{\theta}} \log h_j(\boldsymbol{\theta}) &= \frac{\nabla_{\boldsymbol{\theta}} h_j(\boldsymbol{\theta})}{h_j(\boldsymbol{\theta})} \\ &= \frac{2r_j - 1}{h_j(\boldsymbol{\theta})} [(1 - 2\rho) \mathbf{f}_j \pi_j(\boldsymbol{\theta})(1 - \pi_j(\boldsymbol{\theta}))], \end{aligned}$$

where $\mathbf{f}_j = (1, f_{j,1}, \dots, f_{j,T})^\top$, and so the gradient for the expression in (21) is then

$$\nabla_{\boldsymbol{\theta}} \sum_{j=1}^J \log h_j(\boldsymbol{\theta}) = (1 - 2\rho) \sum_{j=1}^J \mathbf{f}_j \frac{\pi_j(\boldsymbol{\theta})(1 - \pi_j(\boldsymbol{\theta}))}{h_j(\boldsymbol{\theta})}.$$

■

APPENDIX F. PRODUCT MOM NON-LOCAL PRIOR

Figure 8 illustrates the density of the product MOM non-local prior of Johnson and Rossell [2012].

APPENDIX G. COMPUTATIONAL METHODS

G.1. Numerical computation of the marginal likelihood for non-local priors. Briefly, denote by $p^{\text{N}}(\alpha_t | \delta_t = 1, \phi) = \text{N}(\alpha_t; 0, \tau\phi)$ independent Gaussian priors for $t = 1, \dots, T$, and similarly $p^{\text{N}}(\beta_j | \gamma_j = 1, \phi) = \text{N}(\beta_j; 0, \tau\phi)$ for $j = 1, \dots, J$. Proposition 1 in Rossell and Telesca [2017] shows that the following identity holds exactly

$$p(\mathbf{y} | \boldsymbol{\gamma}, \boldsymbol{\delta}) = p^{\text{N}}(\mathbf{y} | \boldsymbol{\gamma}, \boldsymbol{\delta}) \text{E}^{\text{N}} \left[\prod_{t=1}^T \frac{\alpha_t^2}{\tau\phi} \prod_{j=1}^J \frac{\beta_j^2}{\tau\phi} \mid \mathbf{y}, \boldsymbol{\gamma}, \boldsymbol{\delta} \right]$$

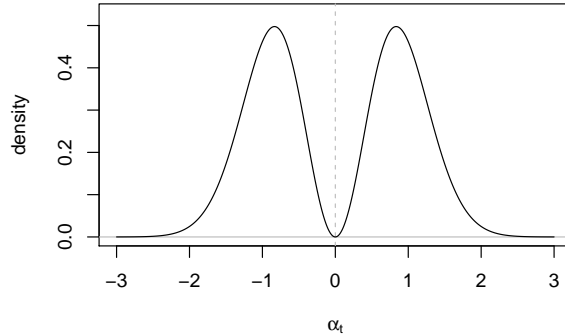


FIGURE 8. Prior density $p(\alpha_t \mid \delta_t = 1, \phi = 1)$ of the MOM non-local prior, with $\tau = 0.348$.

where $p^N(\mathbf{y} \mid \boldsymbol{\gamma}, \boldsymbol{\delta})$ is the integrated likelihood under $p^N(\boldsymbol{\alpha}, \boldsymbol{\beta})$, and $E^N[\cdot]$ denotes the posterior expectation under $p^N(\boldsymbol{\alpha}, \boldsymbol{\beta} \mid \mathbf{y}, \boldsymbol{\gamma}, \boldsymbol{\delta})$. To estimate $p^N(\mathbf{y} \mid \boldsymbol{\gamma}, \boldsymbol{\delta})$ for non-Gaussian outcomes we use a Laplace approximation. Regarding the second term, we approximate it by a product of expectations, which [Rossell et al. \[2021\]](#) showed leads to the same asymptotic properties and typically enjoys better finite- n properties than a Laplace approximation.

G.2. Numerical optimization for empirical Bayes hyper-parameters.

Algorithm 1 describes our method to estimate $\boldsymbol{\theta}^{\text{EP}}$ and $\boldsymbol{\theta}^{\text{EB}}$. We employ the quasi-Newton BFGS algorithm to optimize the objective function. For $\boldsymbol{\theta}^{\text{EB}}$, we use the gradients from Proposition 3.1, while the Hessian is evaluated numerically using line search, with the R function `nlm`. Note, however, that obtaining $\boldsymbol{\theta}^{\text{EB}}$ requires sampling models from their posterior distribution for each $\boldsymbol{\theta}$, which is impractical, to then obtain posterior inclusion probabilities required by (9). Instead, we restrict attention to the models M sampled for either $\boldsymbol{\theta} = \mathbf{0}$ or $\boldsymbol{\theta} = \boldsymbol{\theta}^{\text{EP}}$ in order to avoid successive MCMC runs at every step, relying on the relative regional proximity between the starting point $\boldsymbol{\theta}^{\text{EP}}$ and $\boldsymbol{\theta}^{\text{EB}}$. This proximity would ensure that M contains the large majority of models with non-negligible posterior probability under $\boldsymbol{\theta}^{\text{EB}}$. For $\boldsymbol{\theta}^{\text{EP}}$, we use employ the same BFGS strategy using gradient computed in E.2, with numerical evaluation of the Hessian. This computation requires only one MCMC run at $\boldsymbol{\theta} = \mathbf{0}$, which allows us to use grid search to avoid local optima. As for the size of the grid, we let the user specify what points are evaluated. For K points in the grid one must evaluate the log objective function K^{T+1} times, so we recommend to reduce the grid density as T grows. By default, we evaluate every integer in the grid assuming T is not large, but preferably we avoid coordinates greater than 10 in absolute value, as in our experiments it is very unlikely that any global posterior mode far from zero is isolated, i.e. not reachable by BFGS by starting to its closest point in the grid. Additionally, even

if that were the case, numerically it makes no practical difference, considering that marginal inclusion probabilities are bounded away from zero and one regardless.

Algorithm 1: Obtaining estimates for $\boldsymbol{\theta}^{\text{EP}}$ and $\boldsymbol{\theta}^{\text{EB}}$

Output: Estimates for $\boldsymbol{\theta}^{\text{EP}}$ and $\boldsymbol{\theta}^{\text{EB}}$

- 1: Obtain B posterior samples $(\boldsymbol{\gamma}, \boldsymbol{\delta})^{(b)} \sim p(\boldsymbol{\gamma}, \boldsymbol{\delta} \mid \mathbf{y}, \boldsymbol{\theta} = \mathbf{0})$ for $b = 1, \dots, B$. Denote by $M^{(0)}$ the corresponding set of unique models.
 - 2: Compute $s_t = P(\delta_t = 1 \mid \mathbf{y}, \boldsymbol{\theta} = \mathbf{0})$ and $r_j = P(\gamma_j = 1 \mid \mathbf{y}, \boldsymbol{\theta} = \mathbf{0})$.
 - 3: Conduct a grid search for $\boldsymbol{\theta}^{\text{EP}}$ around $\boldsymbol{\theta} = \mathbf{0}$. Optimize (14) with the BFGS algorithm initialized at the grid's optimum.
 - 4: Obtain B posterior samples $(\boldsymbol{\gamma}, \boldsymbol{\delta})^{(b)} \sim p(\boldsymbol{\gamma}, \boldsymbol{\delta} \mid \mathbf{y}, \boldsymbol{\theta} = \boldsymbol{\theta}^{\text{EP}})$. Denote by $M^{(1)}$ the corresponding set of unique models. Set $M = M^{(0)} \cup M^{(1)}$.
 - 5: Initialize search for $\boldsymbol{\theta}^{\text{EB}}$ at $\boldsymbol{\theta}^{\text{EP}}$. Use the BFGS algorithm to optimize (13), restricting the sum to $(\boldsymbol{\delta}, \boldsymbol{\gamma}) \in M$.
-

APPENDIX H. SUPPLEMENTARY RESULTS

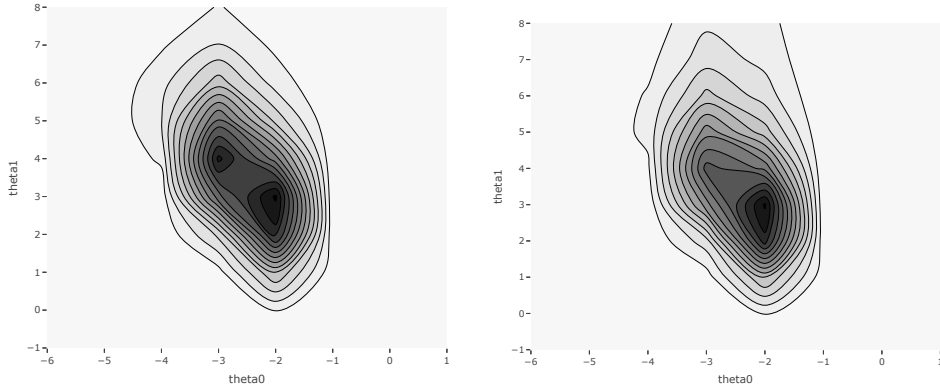


FIGURE 9. Empirical Bayes (left) and Expectation-Propagation (right) objective functions (13) and (14) in the single treatment case ($T = 1$). Here, $\boldsymbol{\theta}^{\text{EB}} = (-2.43, 3.19)$ and $\boldsymbol{\theta}^{\text{EP}} = (-2.34, 3.09)$, for $n = 100$ and $J = 49$, for the first data realization for the simulation design displayed in the center-left panel of Figure 1 with three confounders. See Section 4.1 for further details.

H.1. Illustration of the EB and EP objective functions. Figure 9 shows the Empirical Bayes objective function in (13) and (14) in a simulated dataset with a single treatment. A bimodality is appreciated in the left panel.

H.2. Salary survey: obtention and pre-processing of CPS microdata. Current Population Surveys are administered monthly by the U.S. Bureau of the Census to over 65,000 households. The resulting microdata is made freely available to the public by the Integrated Public Use Microdata Series (IPUMS) website upon registration at:

- <https://cps.ipums.org/cps/>

We manually download the data including all indicators available for 03-2010 and 03-2019, which include data from the Annual Social and Economic Supplement. All transformations necessary to undertake the different analyses presented in this article are openly accessible at:

- https://github.com/mtorrens/cil_article

The user is advised to carefully read the `README.md` file before replicating the analyses. For the CPS raw data pre-processing, we refer to the two scripts created to perform said tasks (in the appropriate order):

- `source/04a_cps_format.R`
- `source/04b_cps_transform.R`

H.3. Salary survey: generation of augmented datasets. For both amounts $K_1 = 100$ and $K_2 = 200$ of artificial predictors, the simulation protocol is the same. Every artificial covariate $\mathbf{z}_k \in \mathbb{R}^n$, for $k = 1, \dots, 100$ or $k = 1, \dots, 200$ respectively, is simulated to correlate to one individual treatment, according to which subset said covariate is assigned to, correlating only indirectly to the rest of treatments. In particular, we drew elements of \mathbf{z}_k from $z_{i,k} \mid d_{i,t} = 1 \sim N(1.5, 1)$, and $z_{i,k} \mid d_{i,t} = 0 \sim N(-1.5, 1)$, where \mathbf{d}_t denotes the corresponding column in the treatment matrix associated to the given \mathbf{z}_k .

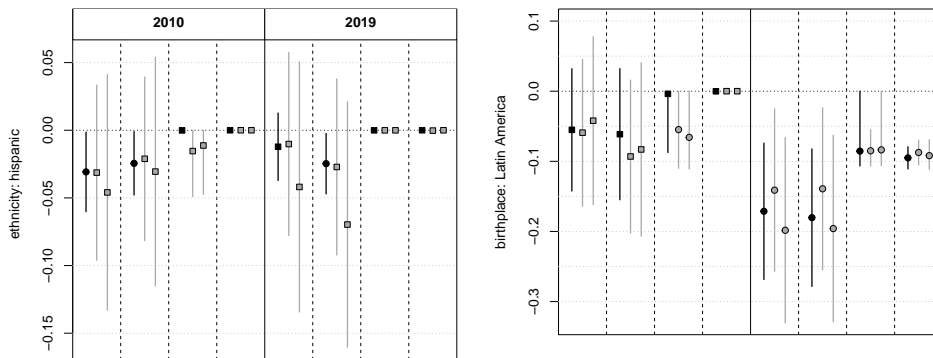


FIGURE 10. Inference for treatment variables “hispanic” (top) and “born in Latin America” (bottom) in 2010 and 2019. Read caption to Figure 4 to read this figure, including method labels (from left to right: OLS, DL, BMA, CIL).

H.4. **Further results on salary survey.** Figure 10 follows Figure 4 by showing the results for the other two treatments: Hispanic ethnicity, and birthplace in Latin America.

H.5. **Further results for abortion data.** This section contains supplementary results for the abortion data analysis. The codes for the variable names follow those of Belloni et al. [2014]. Recall that the main covariates are:

- `prison`: log prisoners per capita
- `police`: log police per capita
- `ur`: unemployment rate
- `inc`: income per capita
- `pov`: poverty rate
- `afdc`: Aid to Families with Dependent Children generosity
- `beer`: beer consumption per capita
- `gun`: presence of concealed weapons law (binary)

The full list of variable names is given in supplementary file `vnames.csv`. The nomenclature can be interpreted as follows:

- Prefix `D` indicates taking the difference between two consecutive years, e.g. `Dprison` is the difference of log prisoners per capita in the current vs. previous year
- Prefix `L` indicates taking a 1-year lagged value, e.g. `Lprison` is last year's log prisoners per capita
- Suffix `0` indicates the initial value of the variable, e.g. `prison0` is the initial log prisoners per capita
- Concatenating variable names with a `.` indicates interactions, e.g. `Dprison.Dur` is the interaction (product) between `Dprison` and `Dur`
- Linear interactions are indicated by `*`, e.g. `Dprison*t` is the interaction (product) between `Dprison` and `time`
- Suffix `Bar` indicates the state-level average, e.g. `prisonBar` is the state's average log prisoners per capita
- `xV0`, `xP0`, `xM0`: initial violent crime, property crime and murder (respectively)
- `DxV0`, `DxP0`, `DxM0`: initial difference in violent crime, property crime and murder (respectively)

We first discuss violent crime. Tables H.5 and 5 show BMA inference for covariates with marginal posterior inclusion probability above > 0.1 in the standard BMA analysis with normal and MOM priors (respectively). In the CIL analyses with normal and MOM priors there are no such covariates. The top model in the BMA-normal, BMA-MOM, CIL-normal and CIL-MOM analysis contained no confounding covariates, and has posterior probabilities of 0.095, 0.305, 0.923 and 0.670 respectively.

TABLE 2. Final DL outcome model for violent crime including covariates found to be related to either the treatment or/outcome. For brevity the intercept and dummy year indicators are omitted

	Estimate	Std. Error	<i>p</i> -value
abortion	−0.21	0.13	0.099
Lpolice	−0.03	0.02	0.184
Dinc0*t	−26.25	38.51	0.496
Dbeer0*t	1.24	0.92	0.181
Linc0*t	−20.31	23.42	0.386
Lprison0 ² *t ²	0.03	0.02	0.234
prisonBar*t	−0.01	0.02	0.453
incBar*t	23.15	24.13	0.338
DxV0*t ²	−0.81	0.38	0.035
xV0	0.36	0.20	0.065

Regarding property crime, the middle panels in Tables H.5 and 5 show results for BMA-Normal and BMA-MOM respectively. Tables 6 and 7 show analogous results for CIL-Normal and CIL-MOM.

Finally, for the murder outcome the results from our CIL methodology are very similar to those from standard BMA. The bottom panels in Tables H.5 and 5 show results for murder under the BMA-Normal and BMA-MOM analyses. The covariate with highest posterior inclusion probability is a term related to the quadratic effect of income. Said covariate is also the only one receiving non-negligible posterior inclusion probability under the CIL analyses (Tables 6-7). In fact, the top model under all analyses contained only this covariate and has a posterior probability of 0.465 for BMA-normal, 0.612 for BMA-MOM, 0.437 for CIL-normal and 0.802 for CIL-MOM.

H.6. Model selection results in simulation study. Figure 11 summarizes model selection results for the simulations described in Figure 1.

H.7. Simulations under growing dimensionality ($T = 1$). Figure 12 studies the effect of growing number of covariates on inference, specifically for $J + T = 25, 100$ and 200 .

H.8. Testing CIL to different amounts of confounders for $T = 1$. Figure 13 shows the effect of having various amounts of active confounders. The results look consistent to the effects reported in Figures 1 and 12, which are magnified for large amounts of active confounders. These are really challenging situations to tackle since the tested methods aim at model sparsity, while the true model size is relatively large. Although our method still performed at oracle rates in low-confounding

TABLE 3. Final DL outcome model for property crime including covariates found to be related to either the treatment or/outcome. For brevity the intercept and dummy year indicators are omitted

	Estimate	Std. Error	p -value
abortion	-0.04	0.04	0.404
Lpolice	-0.02	0.01	0.123
Linc	41.62	9.36	< 0.001
Linc0	-18.25	9.12	0.046
Dinc0*t	-19.77	21.13	0.350
Dbeer0*t	-0.73	0.59	0.214
Linc0*t	222.64	256.72	0.386
Lprison0 ² *t	0.04	0.04	0.314
Linc0 ² *t	-1144.36	1295.88	0.378
Lprison0 ² *t ²	-0.02	0.04	0.567
Lbeer0 ² *t ²	-0.03	0.21	0.878
incBar	-22.22	11.98	0.064
afdcBar	-0.02	0.02	0.125
xP0	0.00	0.03	0.967

TABLE 4. Final DL outcome model for murder including covariates found to be related to either the treatment or/outcome. For brevity the intercept and dummy year indicators are omitted

	Estimate	Std. Error	p -value
abortion	-0.12	0.46	0.800
Lur	-0.35	0.78	0.648
Dur0 ²	1.11	131.86	0.993
Lprison0*t	0.02	0.04	0.696
Linc0*t	0.52	62.67	0.993
Dbeer0*t ²	-0.32	4.07	0.938
incBar*t	-7.48	62.34	0.905
xM0	2.76	3.76	0.464
xM0*t	-4.74	5.85	0.418

scenarios, its relative performance is compromised for the highest levels of confounding. This occurred in part because accurate point estimation in (5) become increasingly harder as the correlation between covariates strengthened, which in turn influenced the ability of the algorithm to calibrate θ reliably. Even in these hard cases, however, its performance is not excessively far to the best competing method, while it clearly outperformed BMA on all of them.

Violent crime				
	$E(\beta_j \mathbf{y})$	2.5%	97.5%	$P(\beta_j \neq 0 \mathbf{y})$
Lpolice	0.00	0.00	0.00	0.12
Dprison*Dur	-0.99	-14.96	0.00	0.12
Dprison*Dur*t	-3.67	-34.15	0.00	0.19
Dprison*Dpov*t	1.05	0.00	10.56	0.19
Dprison*Dpov*t ²	2.30	0.00	13.96	0.25
Dprison0	-0.03	-0.19	0.00	0.22
Property crime				
Lur	-0.06	-0.88	0.00	0.18
Linc	10.61	0.00	48.54	0.33
Linc ²	50.43	0.00	241.44	0.34
Linc0	-2.15	-24.57	0.00	0.18
Linc0 ²	-9.79	-121.24	0.00	0.17
incBar	-11.27	-42.48	0.00	0.26
afdcBar	0.00	-0.05	0.00	0.16
incBar ²	-42.53	-208.84	0.00	0.22
afdcBar ²	0.00	-0.03	0.00	0.12
Murder				
Dinc ²	-385429.57	-645172.36	0.00	0.80

TABLE 5. BMA inference (posterior mean, 0.95 interval and inclusion probability) under MOM prior for abortion data. Covariates with posterior marginal inclusion probability > 0.1

Violent crime				
	$E(\beta_j \mathbf{y})$	2.5%	97.5%	$P(\beta_j \neq 0 \mathbf{y})$
Lprison0*t	0.02	0.00	0.15	0.19
prisonBar*t ²	-0.03	-0.21	0.00	0.19
Property crime				
Dinc ²	-305131.21	-674405.53	0.00	0.62
Dinc ² *t	-409899.71	-3635820.19	0.00	0.15
Dinc ² *t ²	396962.96	0.00	3846788.32	0.12
Murder				
Dinc ²	-305131.21	-674405.53	0.00	0.62
Dinc ² *t	-409899.71	-3635820.19	0.00	0.15
Dinc ² *t ²	396962.96	0.00	3846788.32	0.12

REFERENCES

Joseph Antonelli and Francesca Dominici. Bayesian model averaging in causal inference. In Mahlet G. Tadesse and Marina Vannucci, editors, *Handbook of Bayesian Variable Selection*, chapter 9, pages

TABLE 6. CIL inference (posterior mean, 0.95 interval and inclusion probability) under normal prior for abortion data. Covariates with posterior marginal inclusion probability > 0.1 for property crime and murder (there are none for violent crime)

Property crime				
	$E(\beta_j \mathbf{y})$	2.5%	97.5%	$P(\beta_j \neq 0 \mathbf{y})$
Linc0*t	-2.03	-14.13	0.00	0.22
Murder				
Dinc ²	-227669.02	-614607.65	0.00	0.48

TABLE 7. CIL inference (posterior mean, 0.95 interval and inclusion probability) under MOM prior for abortion data. Covariates with posterior marginal inclusion probability > 0.1 for property crime and murder (there are none for violent crime)

Property crime				
	$E(\beta_j \mathbf{y})$	2.5%	97.5%	$P(\beta_j \neq 0 \mathbf{y})$
afdcBar ² *t	-0.01	-0.07	0.00	0.38
incBar ² *t ²	-40.58	-97.31	0.00	0.40
Murder				
Dinc ²	-91217.96	-604869.53	0.00	0.18

- 201–226. Chapman and Hall/CRC, 1st edition, December 2021. [2](#)
- Joseph Antonelli, Giovanni Parmigiani, and Francesca Dominici. High-dimensional confounding adjustment using continuous spike and slab priors. *Bayesian Analysis*, 14(3):805–828, 09 2019. doi: 10.1214/18-BA1131. [5](#)
- Peter L. Bartlett, Philip M. Long, Gábor Lugosi, and Alexander Tsigler. Benign overfitting in linear regression. *Proceedings of the National Academy of Sciences*, 117(48):30063–30070, 2020. ISSN 0027-8424. doi: 10.1073/pnas.1907378117. [9](#)
- Alexandre Belloni, Victor Chernozhukov, and Christian Hansen. Inference on treatment effects after selection among high-dimensional controls. *Review of Economic Studies*, 81(2):608–650, 2014. [3](#), [4](#), [5](#), [13](#), [14](#), [20](#), [21](#), [22](#), [27](#), [35](#)
- Alberto Caron, Gianluca Baio, and Ioanna Manolopoulou. Estimating Individual Treatment Effects using Non-Parametric Regression Models: a Review. *Journal of the Royal Statistical Society Series A: Statistics in Society*, 185(3):1115–1149, 03 2022. ISSN 0964-1998. doi: 10.1111/rssa.12824. [2](#)
- Ismaël Castillo and Aad van der Vaart. Needles and Straw in a Haystack: Posterior concentration for possibly sparse sequences. *The Annals of Statistics*, 40(4):2069–2101, 2012. doi: 10.1214/

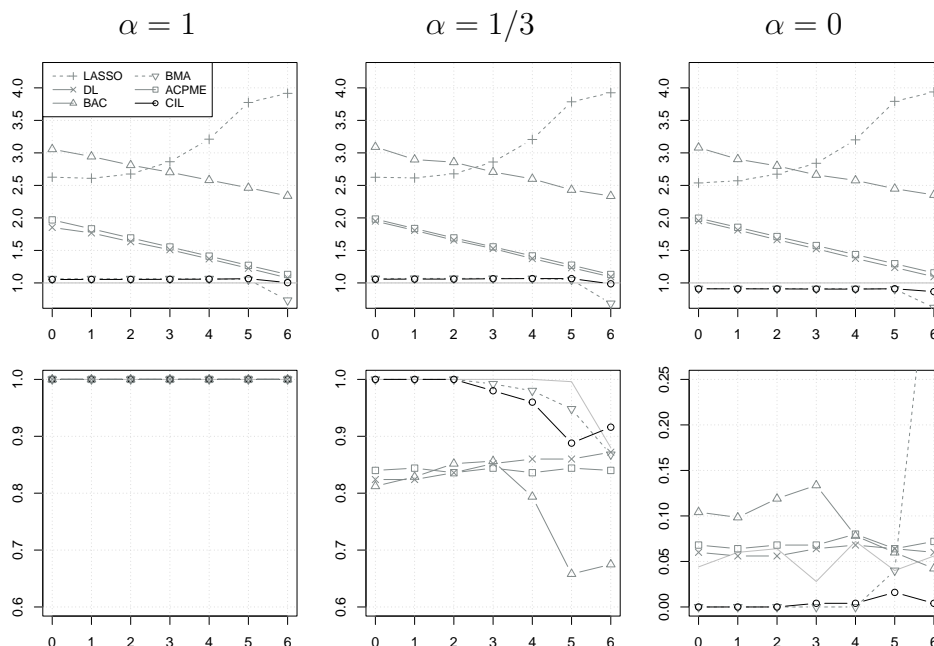


FIGURE 11. To be read vertically in relation to Fig. 1. The top panels show the average outcome model size across levels of confounding, divided by the true model size (i.e. 1 indicates that it matches the true model size). The bottom panels show the probability of selecting the treatment using a 0.05 p -value cut-off for DL, and for Bayesian methods the treatment is included when marginal posterior inclusion probability is $>1/2$. The LASSO does not appear in these panels as its not designed for inference.

12-AOS1029. 8

Victor Chernozhukov, Chris Hansen, and Martin Spindler. hdm: High-dimensional metrics. *R Journal*, 8(2):185–199, 2016. URL <https://journal.r-project.org/archive/2016/RJ-2016-040/index.html>. 14

Victor Chernozhukov, Whitney K Newey, and Rahul Singh. Automatic debiased machine learning of causal and structural effects. In *arXiv:1809.05224*, 09 2018. 4

Merlise A. Clyde and Joyee Ghosh. Finite population estimators in stochastic search variable selection. *Biometrika*, 99(4):981–988, 2012.

11

Xavier De Luna, Ingeborg Waernbaum, and Thomas S Richardson. Covariate selection for the nonparametric estimation of an average treatment effect. *Biometrika*, 98(4):861–875, 2011. 3

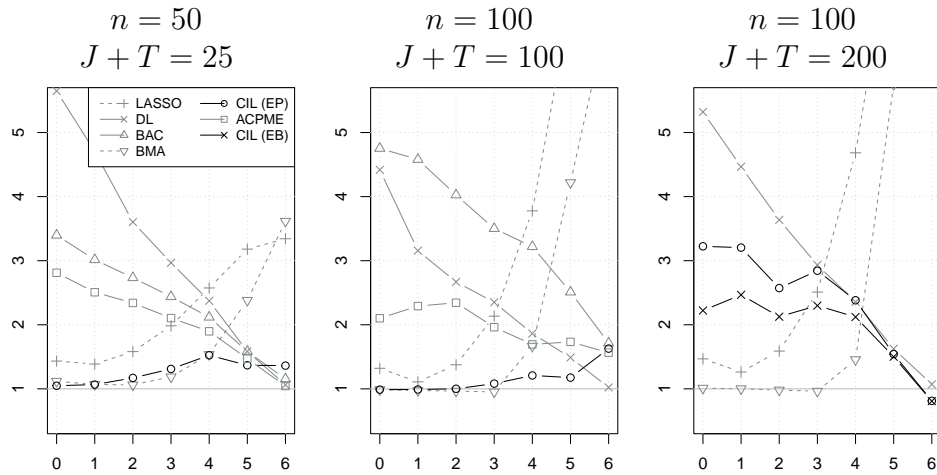


FIGURE 12. Single treatment parameter RMSE (relative to oracle OLS) based on $R = 250$ simulated datasets for each level of confounding. In all panels, $\alpha = 1$ and $|\gamma|_0 = 6$. We show the empirical Bayes version CIL only in the right panel, for the other panels results are undistinguishable relative to EP.

- John J Donohue III and Steven D Levitt. The impact of legalized abortion on crime. *The Quarterly Journal of Economics*, 116(2): 379–420, 2001. [13](#), [20](#), [22](#), [23](#)
- Ashkan Ertefaie, Masoud Asgharian, and David Stephens. Variable selection in causal inference using a simultaneous penalization method. *Journal of Causal Inference*, 6:20170010, 11 2015. doi: 10.1515/jci-2017-0010. [4](#)
- Max H. Farrell. Robust inference on average treatment effects with possibly more covariates than observations. *Journal of Econometrics*, 189:1–23, 06 2015. [4](#)
- Sarah Flood, Miriam King, Renae Rodgers, Steven Ruggles, and J. Robert Warren. Integrated public use microdata series, current population survey: Version 8.0 [dataset]. <https://doi.org/10.18128/D030.V8.0>, 2020. Minneapolis, MN: IPUMS. Accessed: 2021-01-13. [17](#)
- Jerome Friedman, Trevor Hastie, and Robert Tibshirani. Regularization paths for generalized linear models via coordinate descent. *Journal of Statistical Software*, 33(1):1–22, 2010. [14](#)
- Edward I. George and Dean P. Foster. Calibration and empirical Bayes variable selection. *Biometrika*, 87(4):731–747, 12 2000. doi: 10.1093/biomet/87.4.731. [11](#)
- P. Richard Hahn, Carlos M. Carvalho, David Puelz, and Jingyu He. Regularization and Confounding in Linear Regression for Treatment

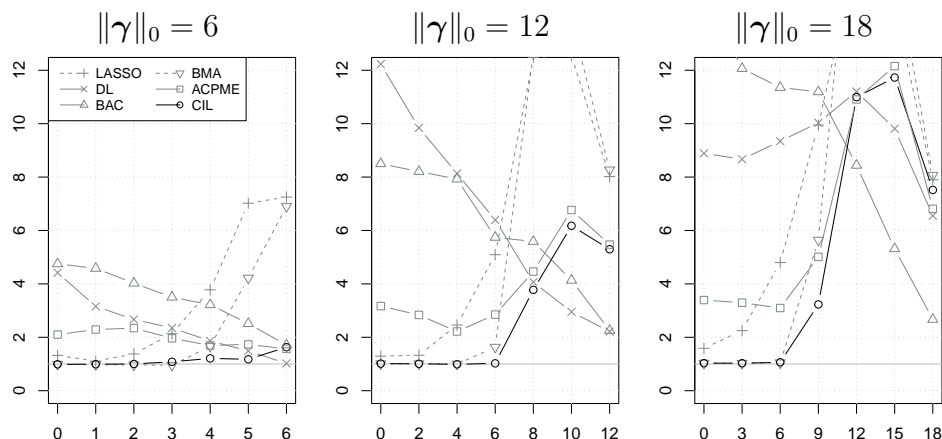


FIGURE 13. Single treatment parameter RMSE (relative to oracle OLS) based on $R = 250$ simulated datasets for each level of confounding reported, as described in Figure 1. In all panels, $n = 100$, $J + T = 100$ and $\alpha = 1$. Sudden general improvement at the right end of center and right panels is due to a sharper deterioration of oracle OLS RMSE at complete confounding relative to other methods.

Effect Estimation. *Bayesian Analysis*, 13(1):163–182, 2018. doi: 10.1214/16-BA1044. 5

Paul Hahn, Jared Murray, and Carlos Carvalho. Bayesian regression tree models for causal inference: Regularization, confounding, and heterogeneous effects. *Bayesian Analysis*, 15(3):965–1056, 09 2020. doi: 10.1214/19-BA1195. 5

Leonard Henckel, Emilija Perković, and Marloes H Maathuis. Graphical criteria for efficient total effect estimation via adjustment in causal linear models. *Journal of the Royal Statistical Society Series B: Statistical Methodology*, 84(2):579–599, 2022. 4

Daniel Hernández-Lobato, José Miguel Hernández-Lobato, and Pierre Dupont. Generalized spike-and-slab priors for bayesian group feature selection using expectation propagation. *Journal of Machine Learning Research*, 14(23):1891–1945, 2013. 12

Valen E. Johnson and David Rossell. Bayesian model selection in high-dimensional settings. *Journal of the American Statistical Association*, 107(498):649–660, 07 2012. doi: 10.1080/01621459.2012.682536. 7, 31

Geneviève Lefebvre, Juli Atherton, and Denis Talbot. The effect of the prior distribution in the bayesian adjustment for confounding algorithm. *Computational Statistics & Data Analysis*, 70:227–240, 02 2014. doi: 10.1016/j.csda.2013.09.011. 3, 4, 5

- Thomas P. Minka. Expectation propagation for approximate bayesian inference. In *Proceedings of the Seventeenth Conference on Uncertainty in Artificial Intelligence*, UAI'01, pages 362–369, San Francisco, CA, USA, 2001a. Morgan Kaufmann Publishers Inc. ISBN 1558608001. 12
- Thomas P. Minka. *A Family of Algorithms for Approximate Bayesian Inference*. PhD thesis, Massachusetts Institute of Technology, USA, 2001b. AAI0803033. 12
- Sonia Petrone, Judith Rousseau, and Catia Scricciolo. Bayes and empirical Bayes: do they merge? *Biometrika*, 101(2):285–302, 2014. 11
- David Rossell. Concentration of posterior probabilities and normalized l_0 criteria. *Bayesian Analysis*, (to appear), 07 2021. 7, 8
- David Rossell and Donatello Telesca. Nonlocal priors for high-dimensional estimation. *Journal of the American Statistical Association*, 112(517):254–265, 2017. doi: 10.1080/01621459.2015.1130634. PMID: 29881129. 11, 31
- David Rossell, Oriol Abril, and Anirban Bhattacharya. Approximate Laplace approximations for scalable model selection. *Journal of the Royal Statistical Society B*, 83(4):853–879, 2021. 7, 10, 32
- David Rossell, John D. Cook, Donatello Telesca, P. Roebuck, Oriol Abril, and Miquel Torrens-Dinarès. *mombf: Model Selection with Bayesian Methods and Information Criteria*, 2023. URL <https://github.com/davidrusi/mombf>. R package version 3.4.0. 6, 11
- James G. Scott and James O. Berger. Bayes and empirical-Bayes multiplicity adjustment in the variable-selection problem. *The Annals of Statistics*, 38(5):2587–2619, 2010. doi: 10.1214/10-AOS792. 8, 11
- Matthias Seeger, Sebastian Gerwin, and Matthias Bethge. Bayesian inference for sparse generalized linear models. In Joost N. Kok, Jacek Koronacki, Raomon Lopez de Mantaras, Stan Matwin, Dunja Mladenič, and Andrzej Skowron, editors, *Machine Learning: ECML 2007*, pages 298–309, Berlin, Heidelberg, 2007. Springer Berlin Heidelberg. ISBN 978-3-540-74958-5. 12
- Minsuk Shin, Anirban Bhattacharya, and Valen E. Johnson. Scalable bayesian variable selection using non-local prior densities in ultrahigh-dimensional settings. *Statistica Sinica*, 28(2):1053–1078, 2018. 7
- Susan Shortreed and Ashkan Ertefaie. Outcome-adaptive lasso: Variable selection for causal inference. *Biometrics*, 73(4):1111–1122, 03 2017. doi: 10.1111/biom.12679. 4
- Denis Talbot, Geneviève Lefebvre, and Juli Atherton. The bayesian causal effect estimation algorithm. *Journal of Causal Inference*, 3(2):207–236, 2015. doi: doi:10.1515/jci-2014-0035. 4
- Chi Wang. *bacr: Bayesian Adjustment for Confounding*, 2016. URL <https://cran.r-project.org/web/packages/bacr/index>.

- [html](#). R package version 1.0.1. [14](#)
- Chi Wang, Giovanni Parmigiani, and Francesca Dominici. Bayesian effect estimation accounting for adjustment uncertainty. *Biometrics*, 68(3):661–686, 2012. doi: <https://doi.org/10.1111/j.1541-0420.2011.01731.x>. [3](#), [5](#), [14](#)
- Chi Wang, Francesca Dominici, Giovanni Parmigiani, and Corwin Zigler. Accounting for uncertainty in confounder and effect modifier selection when estimating average causal effects in generalized linear models: Accounting for uncertainty in confounder and effect modifier selection when estimating aces in glms. *Biometrics*, 71(3):654–665, 04 2015. doi: [10.1111/biom.12315](https://doi.org/10.1111/biom.12315). [4](#)
- Xiangyu Wang and Chenlei Leng. High dimensional ordinary least squares projection for screening variables. *Journal of the Royal Statistical Society: Series B (Statistical Methodology)*, 78(3):589–611, 2016. [9](#)
- Ander Wilson, Corwin Zigler, Chirag Patel, and Francesca Dominici. Model-averaged confounder adjustment for estimating multivariate exposure effects with linear regression: Model-averaged confounder adjustment for estimating multivariate exposure effects. *Biometrics*, 74(3):1034–1044, 03 2018. doi: [10.1111/biom.12860](https://doi.org/10.1111/biom.12860). [4](#), [9](#), [14](#)
- Andrew Wilson. *regimes: Regression in multivariate exposure settings*, 2023. URL <https://github.com/anderwilson/regimes>. R package version 0.6.41. [14](#)
- Ho-Hsiang Wu. *Nonlocal priors for Bayesian variable selection in generalized linear models and generalized linear mixed models and their applications in biology data*. PhD thesis, University of Missouri–Columbia, 2016. [7](#)
- Minjie Xu, Balaji Lakshminarayanan, Yee Whye Teh, Jun Zhu, and Bo Zhang. Distributed bayesian posterior sampling via moment sharing. In *Proceedings of the 27th International Conference on Neural Information Processing Systems - Volume 2*, NIPS’14, pages 3356–3364, Cambridge, MA, USA, 2014. MIT Press. [12](#)